

**HIGH QUALITY BIO-ETHANOL PRODUCTION USING
DISTILLATION, VAPOR PERMEATION AND
PRESSURE SWING ADSORPTION (PSA)
TECHNIQUES**

Saengduan Pimkaew



**A Thesis Submitted in Partial Fulfillment of the Requirements for
the Degree of Master of Science in Biotechnology
Suranaree University of Technology
Academic Year 2010**

แสงเดือน พิมพ์แก้ว : การผลิตเอทานอลความบริสุทธิ์สูงด้วยเทคนิคผสมระหว่าง การกลั่น การแยกไอน้ำผ่านเยื่อแผ่นและการดูดซับ (HIGH QUALITY BIO-ETHANOL USING DISTILLATION, VAPOR PERMEATION AND PRESSURE SWING ADSORPTION (PSA) TECHNIQUE) อาจารย์ที่ปรึกษา : ผู้ช่วยศาสตราจารย์ ดร. อภิชาติ บุญทาวน, 112 หน้า

การผลิตเอทานอลปราศจากน้ำเป็นที่นิยมเพิ่มมากขึ้น โดยปกติการผลิตเอทานอล หลังจากผ่านกระบวนการหมักโดยจุลินทรีย์แล้วจะต้องผ่านกระบวนการกลั่นเพื่อให้ได้ความเข้มข้นที่สูงขึ้น เป็นร้อยละ 95.6 โดยน้ำหนัก และจะไม่สามารถทำให้ความเข้มข้นของเอทานอลสูงขึ้นไปได้อีก โดยการกลั่นธรรมดาเนื่องจากที่สภาวะความดันปกติ อุณหภูมิ 78 องศาเซลเซียส ความเข้มข้นของเอทานอลจะเกิดเป็นของผสมอะซีโโทโรกับน้ำ ซึ่งกระบวนการทำให้เอทานอลบริสุทธิ์สูงขึ้น จึงต้องใช้ต้นทุนที่สูง ดังนั้นงานวิจัยนี้มีวัตถุประสงค์เพื่อศึกษาการปรับปรุงกระบวนการผลิตเอทานอลที่มีความบริสุทธิ์สูงจากน้ำหมักด้วยเทคนิคผสมระหว่าง การกลั่น การแยกไอน้ำผ่านเยื่อแผ่น และการดูดซับ เมื่อไม่นานมานี้หอกลิ้นเอทานอลประสิทธิภาพสูงได้ถูกพัฒนาขึ้นเป็นที่สำเร็จในหน่วยวิจัยการผลิตเชื้อเพลิงชีวภาพจากชีวมวล ภายในมหาวิทยาลัยเทคโนโลยีสุรนารี เนื่องจากหอกลิ้นที่ประดิษฐ์ขึ้นนี้มีข้อได้เปรียบกว่าหอกลิ้นที่ใช้กันอยู่ทั่วไปในอุตสาหกรรมคือ การลงทุนด้านเครื่องจักรและการใช้พลังงานในการกลั่นลดลง จากการทดสอบประสิทธิภาพการกลั่นที่สภาวะต่าง ๆ ในเบื้องต้นพบว่าปัจจัยหลักที่มีผลต่อความเข้มข้นของเอทานอลในส่วนควบแน่นคือ ความเร็วรอบของใบพัด จากการทดลองพบว่าค่าที่เหมาะสมที่สุดคือ 1000 รอบต่อนาที สามารถกลั่นเอทานอลได้ความบริสุทธิ์สูงถึงร้อยละ 95 โดยน้ำหนัก ซึ่งเป็นความเข้มข้นที่สูงที่สุดที่จะกลั่นได้ หลังจากกลั่นจะมีน้ำผสมอยู่ประมาณร้อยละ 5 โดยน้ำหนัก ดังนั้นจึงต้องมีการแยกน้ำออกจากเอทานอลเพื่อให้ได้เอทานอลที่มีความบริสุทธิ์สูงขึ้น ซึ่งกระบวนการที่ใช้ในการแยกน้ำในงานวิจัยนี้เป็นการรวมเอาข้อดีของทั้งสองระบบมาผนวกเข้าด้วยกัน กระบวนการที่ใช้ในการแยกน้ำหลังจากจุดอะซีโโทโรปคือ การแยกไอน้ำผ่านเยื่อแผ่นและการดูดซับ สำหรับกระบวนการแยกไอน้ำผ่านเยื่อแผ่นได้ศึกษาประสิทธิภาพของการผลิตเอทานอลความบริสุทธิ์สูงโดยใช้เยื่อแผ่นชนิดชอบน้ำ ส่วนกระบวนการดูดซับมีวัตถุประสงค์เพื่อผลิตเอทานอลความเข้มข้นสูงถึงร้อยละ 99.7 โดยน้ำหนัก

ประสิทธิภาพของเยื่อแผ่นในการแยกน้ำออกจากไอผสมของกระบวนการแยกไอน้ำผ่านเยื่อแผ่นนั้นขึ้นอยู่กับความดันไอของสารด้านป้อน อุณหภูมิของโมดูล อัตราการไหลด้าน retentate และความดันด้านสูญญากาศ จากผลการทดลองพบว่าเยื่อแผ่นเชิงประกอบ PAN/PVA และท่อใยกลวงเชิงประกอบสามารถผลิตเอทานอลที่มีความบริสุทธิ์ได้สูงถึงร้อยละ 99 โดยน้ำหนัก แต่อย่างไรก็ตาม ประสิทธิภาพในการแยกน้ำออกจากเอทานอลยิ่งทำได้ยากขึ้นเมื่อต้องการเอทานอลที่มีความ

บริสุทธิ์ที่สูงๆ จากสมการการจำลองทางคณิตศาสตร์ชี้ให้เห็นว่าที่ความเข้มข้นของเอทานอลบริสุทธิ์สูงๆ จำเป็นต้องใช้พื้นที่ของเยื่อแผ่นในการแยกน้ำเพิ่มสูงขึ้น

สำหรับกระบวนการดูดซับ โดยตัวดูดซับความชื้น ได้ศึกษาผลของความเข้มข้นของเอทานอลด้านสายป้อน (ร้อยละ 95-99 โดยน้ำหนัก) และความดันด้านสายป้อน (1-3 บาร์) ต่อการแยกน้ำออกจากเอทานอล พบว่าการดูดซับของน้ำมีประสิทธิภาพสูงขึ้นเมื่อเพิ่มความดันและความเข้มข้นเอทานอลด้านสายป้อน จากการทดลองพบว่าเมื่ออุณหภูมิของคอลัมน์ 145 องศาเซลเซียส ความเข้มข้นของเอทานอลด้านสายป้อนร้อยละ 99 โดยน้ำหนัก และความดันทางด้านสายป้อน 3 บาร์ สามารถผลิตเอทานอลความเข้มข้นสูงถึงร้อยละ 99.99 โดยน้ำหนัก



สาขาวิชาเทคโนโลยีชีวภาพ

ปีการศึกษา 2553

ลายมือชื่อนักศึกษา _____

ลายมือชื่ออาจารย์ที่ปรึกษา _____

ลายมือชื่ออาจารย์ที่ปรึกษาร่วม _____

SAENGDUAN PIMKAEW : HIGH QUALITY BIO- ETHANOL
PRODUCTION USING DISTILLATION, VAPOR PERMEATION AND
PRESSURE SWING ADSORPTION (PSA) TECHNIQUES : ASST. PROF.
APICHAT BOONTAWAN, Ph.D., 112 PP.

ANHYDROUS ETHANOL/DISTILLATION/MOLECULAR SIEVE/PRESSURE
SWING ADSORPTION/VAPOR PERMEATION

The production of anhydrous ethanol is increasing popularly, and ethanol can be recovered from fermentation broth by means of distillation. However, water cannot be completely removed due to the presence of the azeotrope at the concentration of 95.6 wt%, 78 °C, and atmospheric pressure. A major challenge in the design of ethanol dehydration plants is high energy cost. The objective of this work is to improve high quality ethanol production from fermentation broth using forced-mixing distillation, vapor permeation (VP), and pressure swing adsorption (PSA) techniques. Recently, a high efficiency continuous distillation system has been successfully developed in our laboratory. This new type of column has advantages over existing distillation columns in terms of lower construction cost and lower energy input. For forced-mixing distillation, the highest purity ethanol concentration of 95 wt% ethanol could be obtained at the optimum stirrer speed of about 1,000 rpm. The condensed azeotrope was subjected to subsequent dehydration by using VP and PSA techniques. For VP, the dehydration performances of hydrophilic membranes to produce anhydrous ethanol were investigated. Water flux across the selective layer depends on many operating parameters, including partial feed pressure, module temperature, and

retentate flow rate. From the experimental results, a composite polyvinyl alcohol (PVA)/ poly-acrylonitrile (PAN) membrane, and NaA zeolite membrane on asymmetric porous support was able to produce more than 99 wt% ethanol. However, the separation became more difficult at higher ethanol concentration. The mathematical simulation suggested that membrane area increased exponentially with the required purity. For adsorption system, 3-Å type molecular sieve was investigated. The masses of water and ethanol adsorbed were measured for various ethanol concentrations (95-99 wt %), and operating feed partial pressures (1-3 bars). From the experimental results, the adsorbed masses of water increased with increasing feed partial pressure and ethanol feed concentration. At the operating conditions of column temperature at 145 °C, ethanol feed concentration of 99 wt %, and feed pressure at 3 bars, the system obtained the highest purity of ethanol concentration at 99.99 wt %.

School of Biotechnology

Academic Year 2010

Student's Signature _____

Advisor's Signature _____

Co-advisor's Signature _____

ACKNOWLEDGEMENTS

This research thesis would not have been possible without the support of many people. I am extremely grateful to Suranaree University of Technology, Thailand for the partial financial support. I would like to express my sincere thanks to my thesis advisor, Asst. Prof. Dr. Apichat Boontawan for excellent adviser, invaluable help, constant encouragement throughout the course of this research and support from the initial to the final level enabled me to develop an understanding of the subject. I am most grateful for his teaching and advice, not only the research methodologies but also many other methodologies in life. I would not have achieved this far and this thesis would not have been completed without all the support that I have always received from him.

I would like to thank my co-advisor, Asst. Prof. Dr. Sunthorn Kanchanatawee for all of the comments, his discussion and good suggestions. He provides a good guidance for writing of the manuscript, checked and corrected the fault of this thesis especially. Deepest gratitude are also due to all of the teachers; Asst. Prof. Dr. Sunthorn, Asst. Prof. Dr. Aphichat, Dr. Keamwich, Asst. Prof. Dr. Mariena, Dr. Pariyaporn, Prof. Catherine, Drs. Eric, Sophie, etc., who was abundantly helpful and offered valuable assistance, support and guidance. Without whose knowledge and assistance this study would not have been successful.

I would also like to convey my sincerely thank to the Suranaree University of Technology for providing the financial means and laboratory facilities for extending

its support. I would also thank School of Biotechnology, Institute of Agricultural Technology, Suranaree University of Technology members and Staff for the constant reminders and much needed motivation without whom this project would have been a distant reality. Internet, books, computers and all that as my source to complete this project. They also supported me and encouraged me to complete this task.

I most gratefully acknowledge my parents for providing everything, such as money, to buy anything that are related to this research work, their advise, their understanding and endless love, through the duration of my studies which is the most needed for this research.

Special thanks also to all my graduate friends, especially group members; every people in Biofuel Production from Biomass Research Unit, School of Biotechnology, Institute of Agricultural Technology, Suranaree University of Technology and my classmate for sharing the literature, sharing our ideas, their help, encouragement and invaluable assistance. Not forgetting to my best friends who always been there. Lastly, I offer my regards and blessings to all of those who supported me in any respects during the completion of the research thesis.

Saengduan Pimkaew

TABLE OF CONTENTS

	Page
ABSTRACT (THAI).....	II
ABSTRACT (ENGLISH).....	IV
ACKNOWLEDGEMENTS.....	VI
TABLE OF CONTENTS.....	VII
LIST OF TABLES.....	XII
LIST OF FIGURES.....	XVI
LIST OF ABBREVIATIONS.....	XXI
CHAPTER	
I INTRODUCTION	
1.1 Background.....	1
1.2 Research objectives.....	2
1.3 Scope and limitation of the study.....	3
II LITERATURE REVIEW	
2.1 Ethanol.....	5
2.2 Ethanol Distillation.....	9
2.2.1 General Principle.....	9
2.2.2 Partial vaporization and partial condensation.....	11

TABLE OF CONTENTS (Continued)

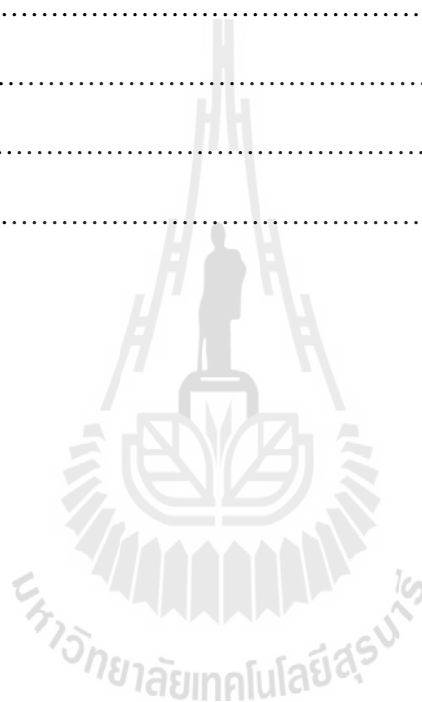
CHAPTER	Page
2.3	Processes for dehydration of Bio-ethanol..... 16
2.3.1	Azeotropic distillation.....16
2.3.2	Membrane separation.....17
2.3.2.1	Mathematical simulation of purity required on membrane21
2.3.3	Pressure Swing Adsorption.....28
III MATERIALS AND METHODS	
3.1	Experimental design.....34
3.2	Materials.....35
3.2.1	forced-mixing distillation.....35
3.2.2	vapor permeation..... 37
3.2.3	Pressure Swing Adsorption.....38
3.2.4	Existing equipments.....39
3.3	Methods.....40
3.3.1	Distillation (forced-mixing distillation).....40
3.3.2	Vapor permeation technique.....42

TABLE OF CONTENTS (Continued)

CHAPTER	Page
3.3.3	Adsorption technique.....44
3.3.4	Hybrid Vapor permeation (NaA zeolite hollow fiber) and Pressure Swing Adsorption system.....45
3.4	Analytical procedures
3.4.1	HYDRANAL® - Moisture Test Kit (Sigma-Aldrich).....47
3.4.2	Density meter (Anton Parr, Austria).....49
3.4.3	Optimization of vapor permeation.....50
IV	RESULTS AND DISCUSSIONS
4.1	Forced-mixing distillation.....52
4.2	Vapor permeation.....55
4.3	Adsorption.....72
4.4	Hybrid vapor permeation and pressure swing adsorption system.....74
V	CONCLUSIONS.....76
REFERENCES.....79	
APPENDICES	
Appendix A.....84	
Appendix B.....85	

TABLE OF CONTENTS (Continued)

CHAPTER	Page
Appendix C.....	86
Appendix D.....	93
Appendix E.....	98
Appendix F.....	104
Appendix G.....	111



LIST OF TABLES

Table	Page
2.1 Physical and chemical properties of ethanol.....	7
2.2 Motor fuel grade ethanol (ASTM International 2004).....	8
A-1 Boiling points of H ₂ O and Ethanol at different pressures.....	84
B-1 Vapor permeation Mathematical simulation of required purity on membrane area.....	85
C-1 Shown distillation results.....	88
D-1 The values of concentration of water, ethanol in retentate and permeate stream, flux and α with cell temperature of polymeric PVA/PAN composite membrane; feed gage pressure (P_g) of 1.4 bar, feed concentration of ethanol 95 wt% and flow rate $0.95 \text{ mL}\cdot\text{min}^{-1}$	91
D-2 The values of concentration of water, ethanol in retentate and permeate stream, flux and α with flow rates of polymeric PVA/PAN-composite membrane; feed gage pressure (P_g) 1.6 bar, feed concentration of ethanol 95 wt% and cell temperature of $120 \text{ }^\circ\text{C}$	92
D-3 The values of concentration of water, ethanol in retentate and permeate stream, flux and α with feed gage pressure (P_g) of polymeric PVA/PAN- composite membrane; flow rate of $1.85 \text{ mL}\cdot\text{min}^{-1}$, feed concentration of ethanol 95 wt% and cell temperature of $120 \text{ }^\circ\text{C}$	93

LIST OF TABLES (Continued)

Table	Page
D-4 The values of concentration of water, ethanol in retentate and permeate stream, flux and α with flow rates of polymeric PVA/PAN-composite membrane; feed gage pressure (P_g) of 0.75 bar, feed concentration of ethanol 95 wt% and cell temperature of 80 °C.....	94
E-1 The values of concentration of water, ethanol in retentate and permeate stream, flux and α with feed gage pressure (P_g) of NaA zeolite tubular membrane; flow rate of 7.785 mL.min ⁻¹ , feed concentration of ethanol 95 wt%, 6 mbar vacuum pressure and cell temperature of 145 °C.....	96
E-2 The values of concentration of water, ethanol in retentate and permeate stream, flux and α with cell temperature of NaA zeolite tubular membrane; feed gage pressure (P_g) 1.6 bar, feed concentration of ethanol 95 wt% and flow rate 8.77 mL.min ⁻¹	97
E-3 The values of concentration of water, ethanol in retentate and permeate stream, flux and α with flow rates of NaA zeolite tubular membrane; feed gage pressure (P_g) 1.6 bar, feed concentration of ethanol 95 wt%, 6 mbar vacuum pressure and cell temperature of 145 °C.....	98
E-4 The values of concentration of water, ethanol in retentate and permeate stream, flux and α with flow rates of NaA zeolite tubular membrane; feed gage pressure (P_g) 1.6 bar, feed concentration of ethanol 95 wt%, 6 mbar vacuum pressure and cell temperature of 120 °C.....	99

IST OF TABLES (Continued)

Table	Page
F-1 The values of concentration of water and ethanol after adsorption with volume (mL); feed concentration of ethanol 95 wt%, column temperature of 145 °C and feed gage pressure 1 bar.....	100
F-2 The values of concentration of water and ethanol after adsorption with volume (mL); feed concentration of ethanol 95 wt%, column temperature of 145 °C and feed gage pressure 1.15 bars.....	101
F-3 The values of concentration of water and ethanol after adsorption with volume (mL); feed concentration of ethanol 95 wt%, column temperature of 145 °C and feed gage pressure 2 bars.....	102
F-4 The values of concentration of water and ethanol after adsorption with volume (mL); feed concentration of ethanol 95 wt%, column temperature of 145 °C and feed gage pressure 3.0 bars.....	103
F-5 The values of concentration of water and ethanol after adsorption with volume (mL); feed concentration of ethanol 97 wt%, column temperature of 145 °C and feed gage pressure 3.0 bars.....	104
F-6 The values of concentration of water and ethanol after adsorption with volume (mL); feed concentration of ethanol 98 wt%, column temperature of 145 °C and feed gage pressure 3.0 bars.....	105

LIST OF TABLES (Continued)

Table	Page
F-7 The values of concentration of water and ethanol after adsorption with volume (mL); feed concentration of ethanol 99 wt%, column temperature of 145 °C and feed gage pressure 3.0 bars.....	106
G-1 The values of concentration of water and ethanol after adsorption with volume (mL); flow rate 19.26 mL.min ⁻¹ and column (PSA), cell (VP) temperature of 145 °C.....	108
G-2 The values of concentration of water and ethanol after adsorption with volume (mL); flow rate 16.1 mL.min ⁻¹ and column (PSA), cell (VP) temperature of 145 °C.....	109
G-3 The values of concentration of water and ethanol after adsorption with volume (mL); flow rate 12.20 mL.min ⁻¹ and column (PSA), cell (VP) temperature of 145 °C.....	110
G-4 The values of concentration of water and ethanol after adsorption with volume (mL); flow rate 4.1 mL.min ⁻¹ and column (PSA), cell (VP) temperature of 145 °C.....	111

LIST OF TABLES (Continued)

Table	Page
D-4 The values of concentration of water, ethanol in retentate and permeate stream, flux and α with flow rates of polymeric PVA/PAN-composite membrane; feed gage pressure (P_g) of 0.75 bar, feed concentration of ethanol 95 wt% and cell temperature of 80 °C.....	94
E-1 The values of concentration of water, ethanol in retentate and permeate stream, flux and α with feed gage pressure (P_g) of NaA zeolite tubular membrane; flow rate of 7.785 mL.min ⁻¹ , feed concentration of ethanol 95 wt%, 6 mbar vacuum pressure and cell temperature of 145 °C.....	96
E-2 The values of concentration of water, ethanol in retentate and permeate stream, flux and α with cell temperature of NaA zeolite tubular membrane; feed gage pressure (P_g) 1.6 bar, feed concentration of ethanol 95 wt% and flow rate 8.77 mL.min ⁻¹	97
E-3 The values of concentration of water, ethanol in retentate and permeate stream, flux and α with flow rates of NaA zeolite tubular membrane; feed gage pressure (P_g) 1.6 bar, feed concentration of ethanol 95 wt%, 6 mbar vacuum pressure and cell temperature of 145 °C.....	98
E-4 The values of concentration of water, ethanol in retentate and permeate stream, flux and α with flow rates of NaA zeolite tubular membrane; feed gage pressure (P_g) 1.6 bar, feed concentration of ethanol 95 wt%, 6 mbar vacuum pressure and cell temperature of 120 °C.....	99

LIST OF FIGURES

Figure	Page
2.1 Cassava fuel ethanol system boundary (Nguyen <i>et al.</i> , 2007).....	6
2.2 Ethanol production pathway (Embden-Meyerhof pathway).....	7
2.3 Column for continuous distillation.....	11
2.4 Temperature composition diagram of ethanol/water binary system at 1 atm (Roehr, 2001).....	12
2.5 Vapor-Liquid Equilibrium diagram (VLE) of EtOH/H ₂ O system at pressure (Warren L. McCabe <i>et.al.</i> , 2005).....	14
2.6 A high efficiency continuous distillation using forced-mixing column (Boontawan A., 2553).....	15
2.7 Schematic diagram of pervaporation system (Huang, 1991).....	19
2.8 Simplified picture of a vapor permeation module, with cross flow on the permeate side of the membrane.....	22
2.9 Boiling points of H ₂ O and Ethanol at different pressures.....	28
2.10 Half cycle for ethanol PSA process (345 s) (steps I.–III.); step IV. represents the switch between the beds (Simo <i>et al.</i> , 2008).....	32
3.1 Setting apparatus of forced-mixing distillation, vapor permeation and pressure swing adsorption.....	35
3.2 SEM images of the composite PVA/PAN membrane.....	37
3.3 Scanning electron microscope photograph of NaA zeolite membrane	38

LIST OF FIGURES (Continued)

Figure	Page
3.4 NaA zeolite tubular membrane.....	38
3.5 Molecular sieves.....	38
3.6 Adsorption bed.....	39
3.7 Diagram of forced-mixing distillation system.....	40
3.8 Schematic diagram of apparatus for vapor permeation.....	42
3.9 Membrane module for vapor permeation technique.....	42
3.10 NaA zeolite tubular membrane construct for vapor permeation technique.....	43
3.11 Setting of apparatus for adsorption technique.....	44
3.12 Schematic diagram of apparatus for pilot plant construction.....	46
3.13 Setting of apparatus for an automatic Karl Fisher titration (Titro Line plus, Schott, Germany).....	47
3.14 Density meter (Anton Paar, Austria).....	49
3.15 Relationship between density and mass fraction of water/ethanol mixture.....	50
4.1 The relationship between stirrer speed and ethanol concentration at different feed flow rates; feed 12 wt% ethanol.....	52
4.2 The relationship between stirrer speed and ethanol concentration at difference feed compositions; flow rate 3.2 mL.min ⁻¹	53

LIST OF FIGURES (Continued)

Figure	Page
4.3 Experimental vapor-liquid equilibrium data for ethanol/water binary system; straight line (-) was 45° line, the open square (□) was the data obtained from simple distillation whilst the curve was generated from equation (1), open circle (○) was the data obtained from our distillation system.....	55
4.4 The compositional evolution in ethanol retentate with proceeding of dehydration at different feed pressures; flow rate 1.85 mL.min ⁻¹ , feed concentration of ethanol 95 wt% and cell temperature of 120 °C.....	56
4.5 The influence of operating feed gage pressure on fluxes and separation factor with 95 wt% of ethanol in the feed side, vacuum 6 mbar, retentate flow rate 1.85 mL.min ⁻¹ , and cell temperature of 120 °C.....	57
4.6 The effect of module temperature on the purity of ethanol in the retentate stream; feed pressure gage 1.4 bars, feed concentration 95 wt% and flow rate 0.95 mL.min ⁻¹	58
4.7 The influence of operating module emperature on fluxes and separation factor with 95 wt% of ethanol in the feed side, vacuum 6 mbar, feed gage pressure 1.4 bars and retentat flow rate 0.95 mL.min ⁻¹	58
4.8 The compositional evolution in ethanol retentate with proceeding of dehydrating at different retentate flow rate; feed pressure gage 1.6 bars, feed concentration of ethanol 95 wt% and cell temperature of 120 °C.....	60

LIST OF FIGURES (Continued)

Figure	Page
4.9 The influence of retentate flow rate on fluxes and separation factor with 95 wt% of ethanol in the feed side, vacuum 6 mbar, feed gage pressure 1.6 bars and cell temperature of 120 °C.....	60
4.10 Effects of feed compositions on total fluxes; 6 mbar vacuum pressure.....	61
4.11 The effect of feed gage pressure on ethanol purity in the retentate; flow rate 7.8 mL.min ⁻¹ , cell temperature of 145 °C, feed concentration of ethanol 95 wt%, and vacuum pressure 6 mbar.....	63
4.12 The influence of operating feed gage pressure on fluxes and separation factor with 95 wt% of ethanol in the feed side, vacuum 6 mbar, retentate flow rate about 7.8 mL.min ⁻¹ , and cell temperature of 145 °C.....	64
4.13 The compositional evolution in ethanol retentate with proceeding of dehydrating at different cell temperature; feed pressure gage 1.6 bars, feed concentration of ethanol 95 wt%, and 6 mbar vacuum pressure.....	65
4.14 The influence of operating cell temperature on fluxes and separation factor with 95 wt% of ethanol in the feed side, vacuum 6 mbar, feed gage pressure 1.6 bars, and retentat flow rate 0.95 mL.min ⁻¹	66
4.15 The compositional evolution in ethanol retentate with proceeding of dehydrating at different retentate flow rates; feed pressure gage 1.6 bars, feed concentration of ethanol 95 wt%, 6 mbar vacuum pressure and cell temperature 145 °C.....	68

LIST OF FIGURES (Continued)

Figure	Page
4.16 The influence of operating retentates flow rate on fluxes and separation factor with 95 wt% of ethanol in the feed side, vacuum 6 mbar, feed gage pressure 1.6 bars and cell temperature 145 °C.....	68
4.17 Effects of feed compositions on total fluxes, 6 mbar vacuum pressure.....	69
4.18 Vapor permeation mathematical simulation of required purity on membrane area.....	70
4.19 The relationship between wt% of water content after adsorption and volume; feed 95 wt% ethanol and column temperature of 145 °C.	72
4.20 The relationship between wt% of water after adsorption and volume; feed gage pressure 3 bars and column temperature of 145 °C.....	73
4.21 Effect of volumetric flow rate on residual water content during dehydration process by using hybrid VP + PSA system. Feed pressure 3 bars, feed ethanol concentration 95 wt%, and temperature 145 °C.....	75

LIST OF FIGURES (Continued)

Figure	Page
4.9 The influence of retentate flow rate on fluxes and separation factor with 95 wt% of ethanol in the feed side, vacuum 6 mbar, feed gage pressure 1.6 bars and cell temperature of 120 °C.....	60
4.10 Effects of feed compositions on total fluxes; 6 mbar vacuum pressure.....	61
4.11 The effect of feed gage pressure on ethanol purity in the retentate; flow rate 7.8 mL.min ⁻¹ , cell temperature of 145 °C, feed concentration of ethanol 95 wt%, and vacuum pressure 6 mbar.....	63
4.12 The influence of operating feed gage pressure on fluxes and separation factor with 95 wt% of ethanol in the feed side, vacuum 6 mbar, retentate flow rate about 7.8 mL.min ⁻¹ , and cell temperature of 145 °C.....	64
4.13 The compositional evolution in ethanol retentate with proceeding of dehydrating at different cell temperature; feed pressure gage 1.6 bars, feed concentration of ethanol 95 wt%, and 6 mbar vacuum pressure.....	65
4.14 The influence of operating cell temperature on fluxes and separation factor with 95 wt% of ethanol in the feed side, vacuum 6 mbar, feed gage pressure 1.6 bars, and retentat flow rate 0.95 mL.min ⁻¹	66
4.15 The compositional evolution in ethanol retentate with proceeding of dehydrating at different retentate flow rates; feed pressure gage 1.6 bars, feed concentration of ethanol 95 wt%, 6 mbar vacuum pressure and cell temperature 145 °C.....	68

LIST OF ABBREVIATIONS

°C	=	Degree Celsius
K	=	Degree Kelvin
%	=	Percent
min	=	Minute
mL	=	Milliliter
cm	=	Centimeter
nm	=	Nanometer
μm	=	Micrometer
Å	=	Angstrom
g	=	Gram
s	=	Second
h	=	Hour
g/mL	=	Gram per Milliliter
kJ/g	=	Kilo joule per Gram
% wt	=	Percent by Weight
mg/L	=	Milligram per Liter
mg/kg	=	Milligram per Kilogram
<i>et.al.</i> ,	=	and others
PVA	=	Poly(vinyl alcohol)
PAN	=	Polyacrylonitrile

LIST OF ABBREVIATIONS (Continued)

P	=	Pressure
T	=	Temperature
N ₂	=	Liquid Nitrogen
<i>J</i>	=	Permeate flux
α	=	Separation factor
kPa	=	Kilopascal
psia	=	Pounds per square inch absolute
rpm	=	Revolutions per minute
SUT	=	Suranaree University of Technology
VLE	=	Vapor-Liquid Equilibrium
ppm	=	Part per million
VP	=	Vapor permeation
PSA	=	Pressure swing adsorption
Min.	=	Minimum
Max.	=	Maximum
[Feed ethanol] _{LM}	=	Logarithmic mean of feed ethanol concentration

CHAPTER I

INTRODUCTION

1.1 Background

Bioethanol is considered a renewable and sustainable fuel for automobiles. Ethanol is the most promising future biofuel due to its high energy value. The ethanol-blended gasoline is marketed under the fuel name, gasohol. It is not only naturally renewable, but gasohol has also lower emissions of carbon monoxide, carbon dioxide and hydrocarbon. The consumption of petroleum-based fuels could also be reduced if the gasohol was used as a motor fuel (Chang *et al.*, 1998). Moreover, anhydrous ethanol is widely used in industries such as organic syntheses, painting, medicine, cosmetics and perfume etc.

One key step in bioethanol production is the removal of a large amount of water from the dilute (<10%) ethanol solution generated by the fermentation process (Wang *et al.*, 2009). Ethanol can be recovered from fermentation broth by means of distillation, but it is commonly known that ethanol forms azeotrope with water at 95.6 weight % ethanol, 78 °C and atmospheric pressure. It is impossible to produce pure ethanol from an azeotropic mixture by normal distillation (at the azeotropic composition the composition of the vapor coming off is the same as that of the liquid). For dehydration of ethanol, there are several methods (Chang *et al.*, 1998).

Optimization of both design and operation variables of a bioethanol purification plant intended to produce fuel-grade ethanol is a challenge to make the

biofuel a realistic alternative in the energy market. While process simulation allows comparing different separation alternatives in terms of energy demand, an optimization-based approach enables the identification of the best configuration for a given superstructure, taking into account both investment and operating costs (Hoch *et al.*, 2008).

Among the methods, the adsorptive option is particularly attractive because of its low energy consumption, which takes up 50–80% of the overall energy required by the fermentative plan (Banat *et al.*, 2000; Hills *et al.*, 1990). Membrane separation as an alternative dehydration process has been developed to replace this energy consuming process. In this work, a commercial composite membrane prepared from modified Poly(vinyl alcohol) (PVA) as a selective layer and polyacrylonitrile (PAN) as a supportive layer will be employed. NaA zeolite hollow fiber which supplied by Mitsui Engineering & shipbuilding, Japan will be investigated. The PVA is often used in the dehydration of water-ethanol mixtures because it exhibits a good hydrophilic property. Vapor permeation (VP) system, were investigated for their dehydration performances in order to produce anhydrous ethanol.

1.2 Research objectives

To study separation process of ethanol from fermentation broth and to further purify its concentration or purity to above 99.7% by weight with the integration of distillation, vapor permeation and pressure swing adsorption techniques.

1.3 Scope and limitation of the study

1.3.1 Distillation (forced-mixing distillation)

1.3.1.1 A high efficiency distillation column has been successfully developed at SUT.

1.3.1.2 The highest purity of ethanol was achieved at 95%.

1.3.2 Vapor permeation

1.3.2.1 To separate ethanol from fermentation broth using vapor permeation technique until ethanol concentration of 99% by weight was achieved.

1.3.2.2 To investigate the effects of operating conditions such as feed temperature, feed pressure, retentate flow rates, module temperature which control dehydration performances with the good of achieving 99% ethanol by weight.

1.3.2.3 To determine key parameters such as the total flux, ethanol flux, water flux and separation factor which indicate the dehydration performances.

1.3.2.4 Application of the composite PVA/PAN membrane in ethanol dehydration is also investigated using vapor permeation experiment.

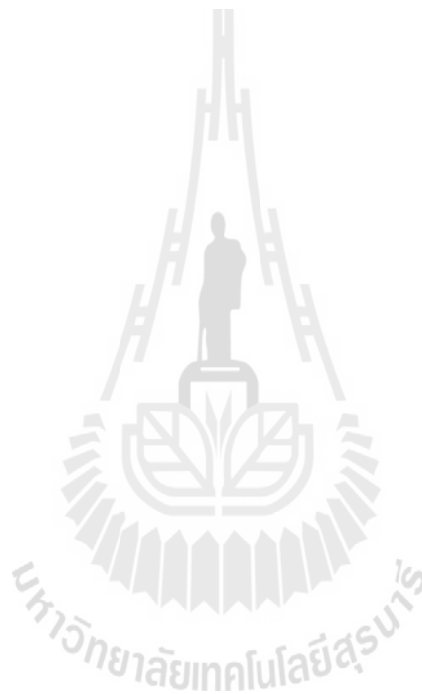
1.3.2.5 To determine the amount of water in the solution mixture of ethanol by using Karl Fischer's titration and density meter.

1.3.2.6 To compare performance of difference hydrophilic membrane module type; plate and frame (composite PVA/PAN membrane) and hollow fiber ceramic membrane.

1.3.3 Pressure Swing Adsorption

1.3.3.1 To separate ethanol from fermentation broth using pressure swing adsorption technique in order to achieve high ethanol concentration or purity with water of less than 0.3% by weight.

1.3.3.2 To investigate the effects of feed composition of ethanol, feed pressure and the volume of ethanol after adsorption with time.



CHAPTER II

LITERATURE REVIEW

2.1 Ethanol

Bioethanol is a two-carbon alcohol that can be produced through the fermentation (sugar cane), starchy biomass (corn), or cellulosic biomass (agricultural or forest wastes). Bioethanol can be used advantageously as a transportation fuel and has therefore been cited as a possible alternative to fossil fuels that could help alleviate environmental and energy dependency problems. Currently most of the world's bioethanol is produced through the fermentation by yeast or bacteria of sugars extracted from sugar cane and corn. The traditional yeast fermentation process is limited to final ethanol concentrations of approximately 10% (by mass) due to product inhibition. The inhibition problem is further exacerbated when genetically modified microorganisms are used to ferment the pentose sugars resulting from the hydrolysis of lignocellulosic biomass. This product inhibition impacts both the efficiency of the fermentation system, since larger fermenters are required, and the efficiency of downstream separation, since a relatively dilute stream must be processed (Haelssi *et al.*, 2008).

In this review, only the cassava fuel ethanol (CFE) was discussed. The system boundary of the cassava fuel ethanol was set up to identify the exchange of the system with the environment in terms of energy inputs and outputs. As shown in

Figure 2.1, the three main segments involved in the CFE system are (1) cassava cultivation/processing, (2) ethanol conversion, and (3) transportation

Ethanol conversion, Various important processes included in this segment, like liquefaction, saccharification, and fermentation, and distillation/dehydration, are presented in Figure 2.1. Treatment of distilled mash produces biogas. Sources of energy consumed to convert cassava starch to ethanol include bunker oil, biogas, and electricity.

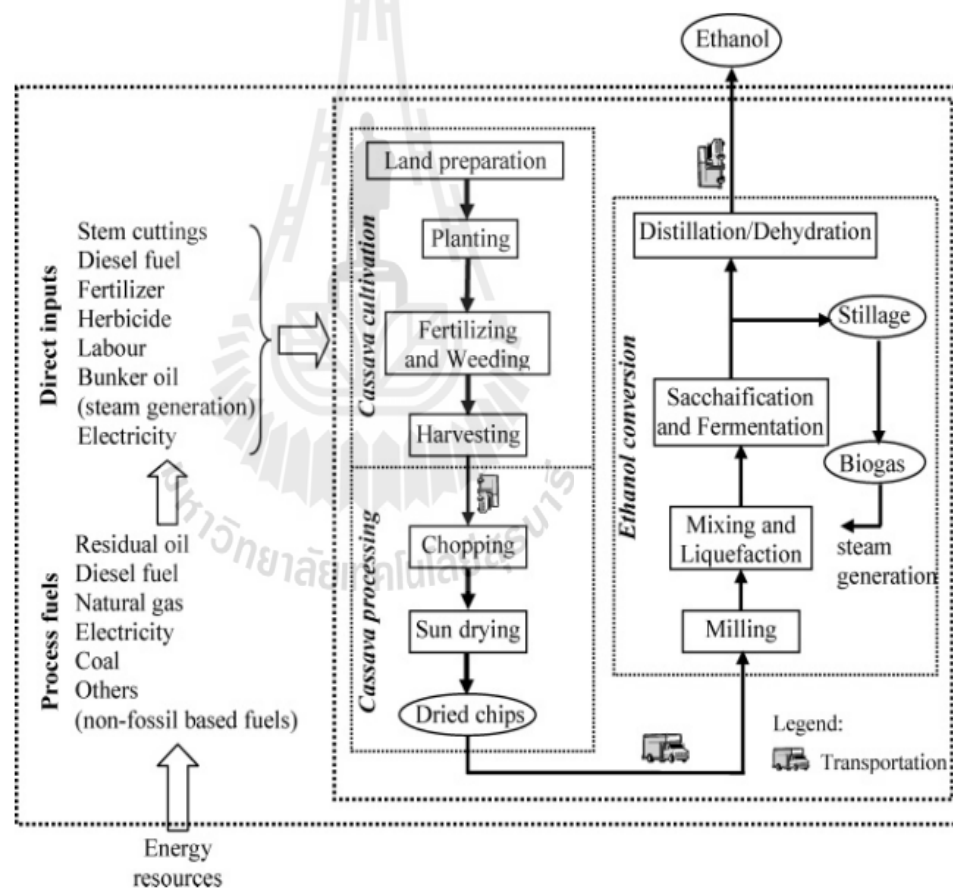


Figure 2.1 Cassava fuel ethanol system boundary (Nguyen *et al.*, 2007).

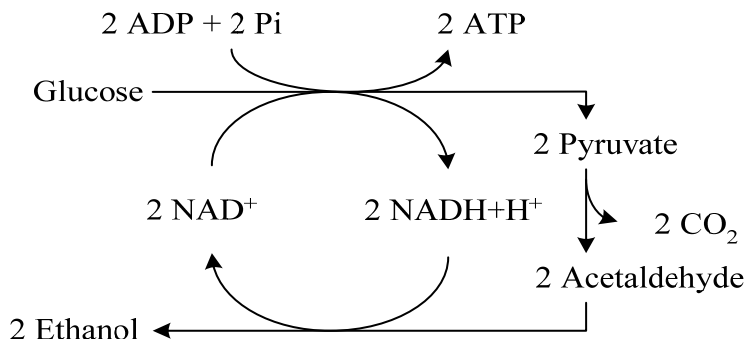


Figure 2.2 Ethanol production pathway (Embden-Meyerhof pathway).

Ethanol Fermentation:



Ethanol can be recovered from fermentation broth by means of distillation, but it is commonly known that ethanol forms an azeotrope with water at 89.4 mole%, (95.6 wt% ethanol), 78 °C and atmospheric pressure. It is impossible to produce pure ethanol from an azeotropic mixture by normal distillation (at the azeotropic composition the composition of the vapor coming off is the same as that of the liquid). Azeotropic distillation is a way to break the azeotrope for production of MFGE and anhydrous ethanol.

Table 2.1 Physical and chemical properties of ethanol.

Properties	
Molecular formula	CH ₃ CH ₂ OH
Molar mass	46
Boiling point at 1 atm	78.32 °C
Density	0.7893g/ml (20 °C)
Heating value of combustion	29.68 kJ/g (25 °C)
Autoignition temperature	793.0 °C

Table 2.2 Motor fuel grade ethanol (ASTM International 2004).

Components	Unit	Min.	Max.	Test Method
Ethanol	wt%	98.7	-	EC/2807/2000 method I
Higher Saturated mono-alcohol	wt%	-	2	EC/2807/2000 method II
Methanol	wt%	-	1	EC/2807/2000 method III
Water	wt%	-	0.3	EN 15489
Inorganic chloride	mg/L	-	20	EN 15484
Copper	mg/kg	-	0.1	EN 15488
Total acidity (as acetic acid)	wt%.	-	0.007	EN 15491
Phosphorus	mg/L	-	0.5	EN 154887
Nonvolatile material	mg/100 mL	-	10	EC/2807/2000 method II
	mg/kg	-	10	EN 15485, EN 15486
pH	-	6.5	9	EN 15490
Appearance	-	Clear and bright		Visual inspection

Ethanol or ethyl alcohol (C_2H_5OH) is a clear colourless liquid, it is biodegradable, low in toxicity and causes little environmental pollution if spilt. The ethanol burns to produce carbon dioxide and water. The ethanol is a high octane fuel and has replaced lead as an octane enhancer in petrol. By blending ethanol with gasoline its can also oxygenate the fuel mixture so it burns more completely and reduces polluting emissions. Ethanol fuel blends are widely sold in the United States. The most common blend is 10% ethanol and 90% petrol (E10). Vehicle engines require no modifications to run on E10 and vehicles warranties are unaffected also.

Only flexible fuel vehicles can run on up to 85% ethanol and 15% petrol blends (E85). Moreover anhydrous ethanol is widely used in many industries, such as painting, medicine, cosmetics, perfume, etc. Recently, lower amount of residual water or anhydrous ethanol has drawn much attention in biodegradable plastic industry as it can be used in esterification technique for purification of lactic acid, the precursor of Polylactic acid (PLA).

2.2 Ethanol Distillation

2.2.1 General Principle

Separation operation achieve their objective by the creation of two or more coexisting zones which differ in temperature, pressure, composition, and/or phase state. Each molecular species in the mixture to be separated reacts in a unique way to differing environments offered by these zones. Consequently, as the system moves toward equilibrium, each species establishes a different concentration in each zone, and this results in a separation between the species. The separation operation called distillation utilizes vapor and liquid phase at essentially the same temperature and pressure for the coexisting zones. Various kinds of devices such as random or structured packings and plats or trays are used to bring the two phases into intimate contact. Trays are stacked one above the other and enclosed in a cylindrical shell to form a column. Packings are also generally contained in a cylindrical shell between hold-down and support plates. A typical-tray distillation column plus major external accessories is shown schematically in Figure 2.3.

The feed material, which is to be separated into fractions, is introduced at one or more points along the column shell. Because of the difference in gravity

between vapor and liquid phases, liquid runs down the column, cascading from tray to tray, while vapor flows up the column, contacting liquid at each tray.

Liquid reaching the bottom of the column is partially vaporized in a heated reboiler to provide boil-up, which is sent back up the column. The remainder of the bottom liquid is withdrawn as bottoms, or bottom product. Vapor reaching the top of the column is cooled and condensed to liquid in the overhead condenser. Part of this liquid is returned to the column as reflux to provide liquid overflow. The remainder of the overhead stream is withdrawn as distillate, or overhead product. In some cases only part of the vapor is condensed so that a vapor distillate can be withdrawn.

This overall flow pattern in a distillation column provides countercurrent contacting of vapor and liquid streams on all the trays through the column. Vapor and liquid phases on a given tray approach thermal, pressure, and composition equilibria to an extent dependent upon the efficiency of the contacting tray.

The lighter (lower-boiling) components tend to concentrate in the vapor phase, while the heavier (higher-boiling) components tend toward the liquid phase. The result is a vapor phase that becomes richer in light components as it passes up the column and a liquid phase that becomes richer in heavy components as it cascades downward. The overall separation achieved between the distillate and the bottoms depends primarily on the relative volatilities of the components, the number of contacting trays, and the ratio of the liquid-phase flow rate to the vapor-phase flow rate.

If the feed is introduced at one point along the column shell, the column is divided into an upper section, which is often called the rectifying section, and a lower section, which is often referred to as the stripping section.

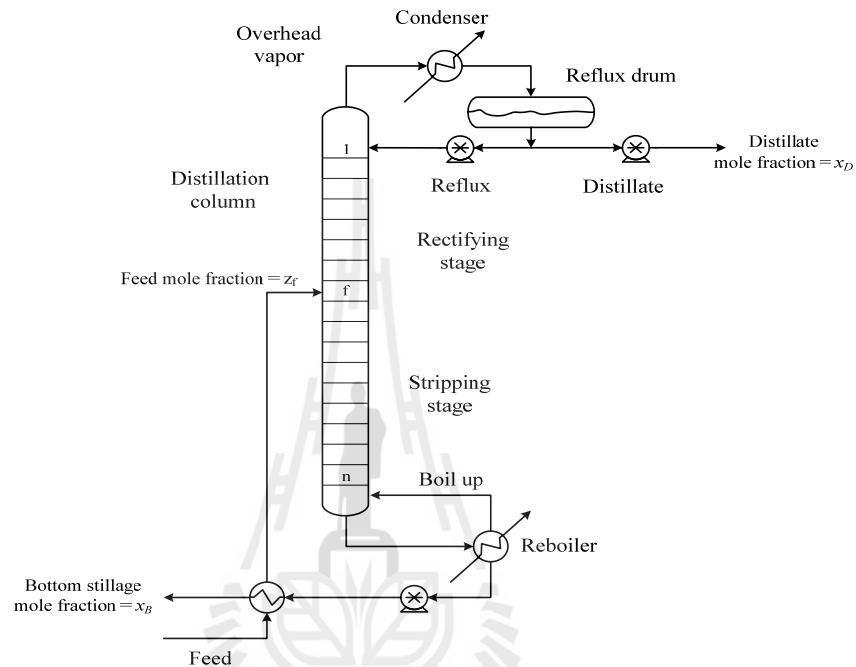


Figure 2.3 Column for continuous distillation.

2.2.2 Partial vaporization and partial condensation

Figure 2.4 shows the equilibrium diagram of ethanol/water binary system, and all compositions are expressed as mole fraction of ethanol in the liquid phase. The lower curve plots the bubble point of the binary mixture as a function of composition whilst the upper curve is the dew point. For a given temperature and composition, this diagram tells the nature and composition of each phase of the mixture that is present.

Thus, if 0.12 mole fraction of ethanol/H₂O is heated in a vessel, closed in such a way that the pressure remains atmospheric and no material can escape and the mole fraction of ethanol is plotted in X axis, and the temperature at which the mixture boil is plotted in Y axis. Point A represents in a sub-cooled region. When temperature (T) reaches 85 °C, the liquid will boil as shown in point B. Some vapor (V) of composition 0.45 mole fraction of Ethanol is formed (point E). Further heating at constant pressure (point C), all liquid will vaporized to give vapor of the original composition (0.12 mole). There is a critical composition (F) where the vapor phase has the same composition as in the liquid phase; therefore, no composition change occurs on boiling. This critical mixture is call azeotropic point which forms at 89.5 mole% or 95.6 wt% ethanol (78.2 °C).

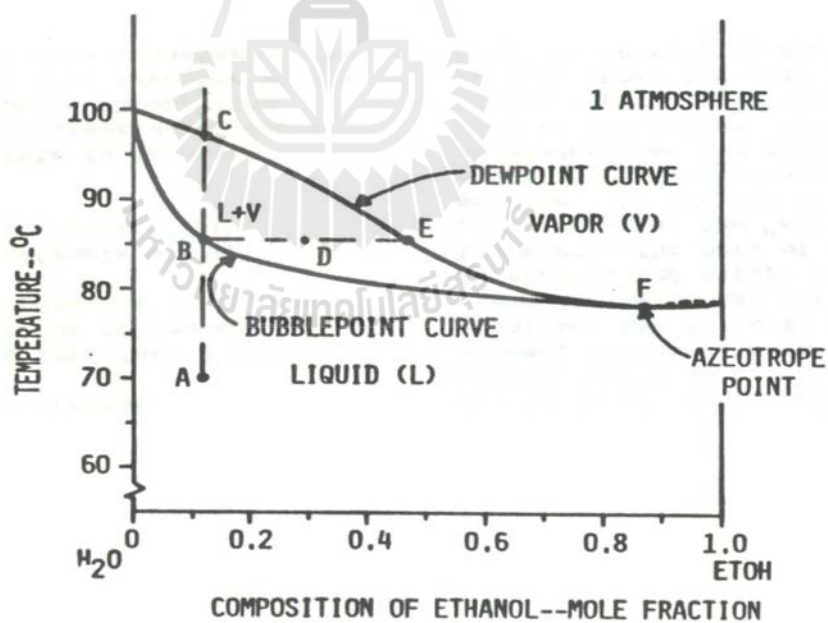


Figure 2.4 Temperature composition diagram of ethanol/water binary system at 1 atm (Roehr, 2001).

Distillation is the oldest method to separate a mixture of compounds based on their difference in volatility. In ethanol distillation processes, separation is carried out in the distillation column in which the vapor going to the upper section get richer in the ethanol concentration, leaving behind the heavier liquid component in the lower section. Part of the liquid descending to the lower column will be in contacted with the raising vapor. The knowledge of vapor-liquid equilibrium (VLE) data is very important to design and maximize distillation performance. Estimation of vapor phase mole fraction of component i (y_i) can be obtained using a relationship (Ohe, S., 1989);

$$y_i P = x_i \gamma_i P_i^{sat} \quad i = 1, 2, \dots, n \quad (1)$$

Where P is the pressure, x_i is the liquid phase mole fraction of component i , γ_i is the activity coefficient calculated by using the UNIQUAC model, and P_i^{sat} is the saturation vapor pressure of component i which can be expressed using Antoine's equation (Fáundez, C.A. *et al.*, 2006).

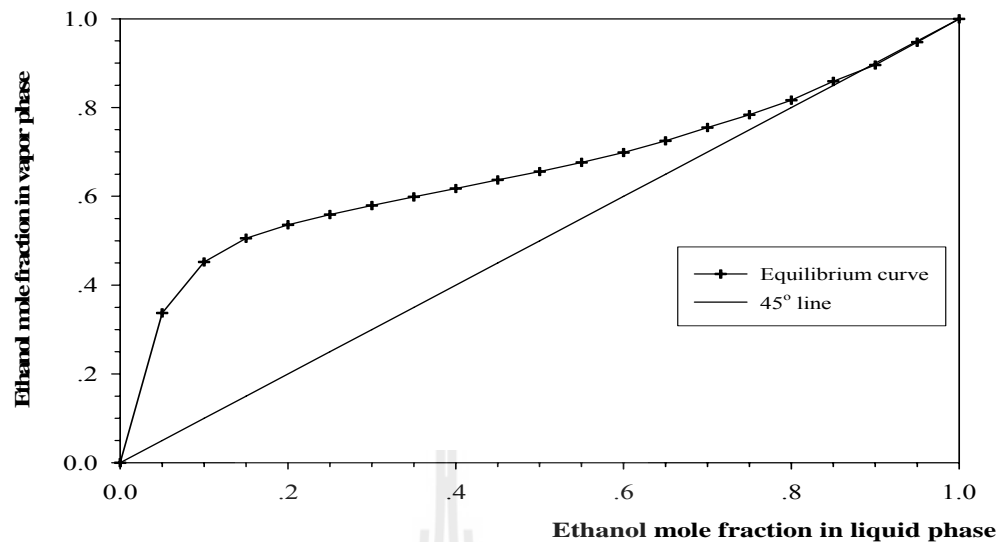


Figure 2.5 Vapor-Liquid Equilibrium diagram (VLE) of ethanol/water system at constant pressure (Warren L. McCabe *et.al.*, 2005).

Although ethanol is highly volatile, separation becomes more difficult especially at lower percentage of water in the vapor phase. Distillation is usually the method of choice for primary separation. However, water cannot be completely removed due to the presence of azeotrope. Continuous fractionating distillation is usually employed; however, the number of stage required to achieve the desired degree of separation is very high (Seader, J.D. and E.J. Henley, 2005). In general, industrial distillation column possesses more than 70 plates in order to achieve 95% purity which results in very high investment cost and difficulty for maintenance. Smaller scale distillation units are not technically and economically feasible. The biofuel production from biomass research unit was established since 2009 with one of the main objectives to carry out research in the field of dehydration of ethanol solutions. By far, the most important breakthrough of the research unit is the construction of a lab scale continuous distillation unit as shown in Figure 2.6.



Figure 2.6 A high efficiency continuous distillation using forced-mixing column (Boontawan A., 2553): 1, motor; 2, condenser; 3, inlet; 4, heat exchanger; 5, speed controller; 6, feed pump; 7, feed solution; 8, product; 9, boiler; 10, ethanol heater.

The working principle is based on forced-mixing of uprising ethanol/water vapor with series of rotating down-flow impellers. A hot plate is used as the main heating device. Fermentation broth is fed via the inlet port located at the middle of the column. The column contains neither plates nor packing materials inside; a center shaft with impellers is instead rotating at a high agitation rate. With an optimum motor speed and heating input, ethanol is evaporated and rises up the rectifying section whereas thin stillage flows down the stripping section. The force-mixing system accelerates vaporization-condensation cycles along the internal wall of the

column which results in extremely rapid equilibrium. The highest ethanol concentration was obtained at 95 wt% for distillation of fermentation broth which is the same quality as industrial scale distillation (Boontawan A., 2553). The system also employs 2 heat exchangers to warm the feed solution as well as to cool down the distillate vapor and thin stillage. Therefore, heat conservation is greatly efficient.

2.3 Processes for dehydration of Bio-ethanol

2.3.1 Azeotropic distillation

Azeotropic distillation is one of a range of techniques used to break an azeotrope in distillation. In chemical engineering, the azeotropic distillation usually refers to the specific technique of adding another component to generate a new, lower-boiling azeotrope that is heterogeneous (e.g. producing two, immiscible liquid phases), such as the example below with the addition of benzene to water and ethanol, high toxicity of chemicals used. In actual fact, this practice of adding an entrainer which forms a separate phase is a specific sub-set of (industrial) azeotropic distillation methods, or combination thereof. The azeotropic distillation process required a high energy input of 10,376 kJ/kg EtOH (Matsuura, 1994) and is no longer economically attractive.

Heterogeneous azeotropic distillation is a widely practiced process for the separation of binary azeotropic mixtures into their pure component constituents. A classic example of heterogeneous azeotropic distillation is the use of benzene to separate water from ethanol. In 1902, Young prepared absolute alcohol from a mixture of ethanol and water using benzene. Several compounds such as benzene, cyclohexane, acetone, and pentane can be used as an entrainer to achieve this

separation. Of these, benzene and cyclohexane have been used most extensively. Presently, benzene is in disuse due to its carcinogenic nature, although it is still being employed in some countries. All existing commercial processes for the dehydration of ethanol try to obtain pure ethanol. This process requires quite a lot of energy because it is necessary to maintain and recirculate high quantities of entrainer throughout the column to achieve the desired azeotropic effect. In addition, pure alcohol must be adequately stored to prevent water from the atmosphere being absorbed by it. Instead of obtaining absolute ethanol, it is possible to directly attain a “dry” mixture of ethanol + hydrocarbon, utilizing less energy. In this case, the high concentrations of entrainer necessary to circulate throughout the column are achieved by new input streams of the hydrocarbon and not by its vaporization/condensation. The ethanol and hydrocarbon mixture thus obtained may be employed as an additive to gasoline without the need of subsequent distillation. Many of the constituents of gasoline may be used as entrainers in the dehydration of alcohol by azeotropic distillation (Gomis *et al.*, 2007).

2.3.2 Membrane separation

Membrane processes are becoming more important in this era of escalating energy costs because they typically require much less energy than alternative separation methods such as distillation. Gas permeation using membranes is widely used for separating mixtures such as oxygen/nitrogen, hydrogen/carbon dioxide, methane/nitrogen, etc. These gaseous membrane systems operate essentially isothermally because there are no phase changes. There are several types of liquid membrane systems (Luyben., 2009).

Pervaporation (PV) and vapor permeation (VP) are membrane processes suitable for separating multinary organic mixtures, in particular azeotropes, where conventional separation techniques are fail. Both membrane processes are closely related to one another differing only so far that the feed is a liquid and a vapor mixture respectively while the permeate in both cases is vaporous. The thermodynamic driving force for the material transport through the nonporous membrane is given by the difference in the chemical potential of the individual permeating components between the feed and the permeate side, usually achieved by a low permeate pressure. Compared to pervaporation vapor permeation has the advantage that no phase transition occurs between feed and permeate, i.e. the problems going along with supplying the enthalpy of evaporation are avoided. For the same operating conditions, the use of a liquid feed mixture in pervaporation and the corresponding equilibrium feed vapor in vapor permeation has the consequence that the same differences in the chemical potential for all permeating components are given in both processes. Having the same driving force similar separation characteristics are to be expected (Schehlmann *et al.*, 1995).

In recent years pervaporation has emerged as an energy-efficient and highly selective separation process for the separation of volatile products and for the dehydration of organic chemicals. Also the productivity and conversion rate can be significantly increased when reaction is coupled with PV, i.e. a PV reactor. Pervaporation involves the use of a liquid feed to produce a vapor permeate and a liquid retentate. In pervaporation, the separation of two or more components across a membrane takes place by differing rates of diffusion through a thin polymer and an

evaporative phase change comparable to a simple flash step. A concentrate and vapor pressure gradient is used to allow one component to preferentially permeate across the membrane. A vacuum applied to the permeate side is coupled with the immediate condensation of the permeate vapors (Wasewar *et al.*, 2009). As shown in Figure 2.7, the transport mechanism for the pervaporation system can be explained using the solution-diffusion model which involves three major steps. The first step involves absorption of chemical molecules into the membrane surface. The second step is the diffusion across the membrane matrix due to concentration and/or pressure difference. The last step is desorption, the chemical compound then vaporizes somewhere in the membrane, and can be obtained as a vapor under vacuum or swept out by an inert carrier gas before being collected in a cold trap. Separation of the fluid mixture can be successfully achieved with a selection of membranes exhibiting both high permeation rate and good selectivity (Delgado *et al.*, 2008).

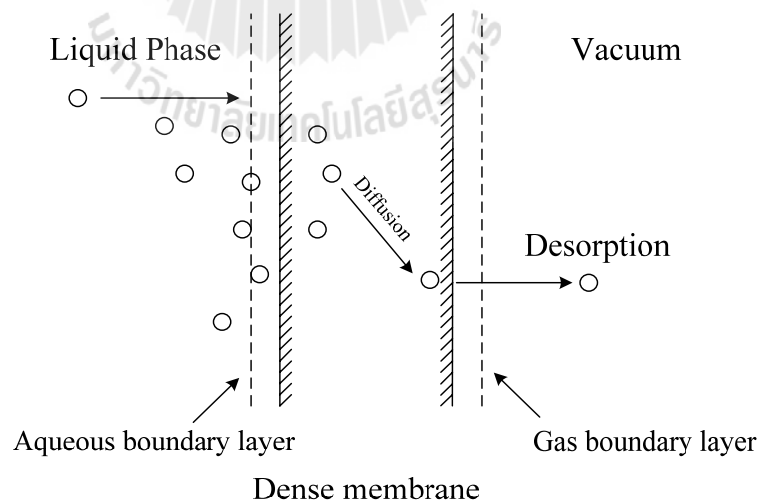


Figure 2.7 Schematic diagram of pervaporation system (Huang, 1991).

In PV system, the feed side is in a form of liquid whilst the feed is applied as a vapor phase for the latter case. In VP system, the separating component just has to permeate through the membrane therefore the problem of supplying the heat of vaporization can be avoided. In addition, the system seems to be suitable to separate water at the top of fractionation columns where the vapor feed can be supplied directly to the membrane module (Yeom *et al.*, 1997).

The membrane performance can be described by permeate flux J ($\text{kg}\cdot\text{m}^{-2}\cdot\text{h}^{-1}$) and separation factor α which can be defined as follow;

$$J = \frac{W}{At} \quad (2)$$

Where W is the weight of the permeate (kg), A is the membrane area (m^2), and t is the time (h), respectively.

$$\alpha = \frac{w_{f,\text{water}}/w_{p,\text{water}}}{w_{f,\text{ethanol}}/w_{p,\text{ethanol}}} \quad (3)$$

Where, w_f and w_p are the weight fraction of water and ethanol in the feed and permeate side, respectively. Based on the solution-diffusion model, the mass transport of component in pervaporation system, i ($\text{mole}\cdot\text{s}^{-1}$) can be written in terms of the difference in partial pressure as followed,

$$m_{i,p} = A \cdot Q_i \cdot \Delta p_i \quad (4)$$

Where A is the membrane area (m^2),

Q_i is the permeance ($\text{mol}\cdot\text{m}^{-2}\cdot\text{s}^{-1}\cdot\text{Pa}^{-1}$),

Δp_i is the driving force across the membrane (Pa) which can be expressed as followed,

$$\Delta p_i = x_{i,f} \cdot \gamma_i \cdot P_f^* - x_{i,p} \cdot P_p \quad (5)$$

Where $x_{i,f}$ is the mole fraction of component i in the feed side,

γ_i is the activity coefficient of i in the feed side determined using UNIQUAC equation,

P_f^* is the saturated vapor pressure of i estimated by Antoine vapor pressure equation,

$x_{i,p}$ is the mole fraction of i in the permeate side,

P_p is the permeate pressure, respectively (Ried, R.C. *et al.*, 2000).

In vapor permeation, the Δp_i of equation (5) is the difference in partial vapor pressure of i between feed ($p_{i,f} = x_{i,f} \cdot P_f$) and permeate side ($p_{i,p} = x_{i,p} \cdot P_p$), where P_f is the total feed pressure. Water can be successfully separated from ethanol/water mixture in order to produce motor fuel grade ethanol using both PV and VP systems. Comparing PV and VP processes, the results suggest that VP has advantages over PV system in terms of separation performances (Boontawan *et al.*, 2007).

2.3.2.1 Mathematical simulation of purity required on membrane

area: The following diffusion model for vapor permeation module is used (Torbjorn *et al.*, 1995):

The main problem in modeling vapor permeation processes is to describe the mass transport across the membrane. The reason is the

coupling between the transport properties of the different species present in the feed; i.e. the permeability of each component is concentration dependent. The permeability is also a function of the pressures and temperature in the system. The main assumptions in this design model are:

1. Negligible pressure-drop along either side of the membrane surface
2. Constant temperature in the membrane module
3. Plug-flow along the feed side of the membrane
4. Cross-flow along the permeate side of the membrane

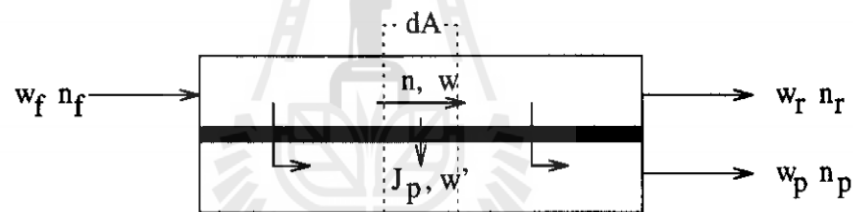


Figure 2.8 Simplified picture of a vapor permeation module, with cross-flow on the permeate side of the membrane.

Figure 2.8 shows a simplified picture of a vapor permeation module for the separation of a binary mixture. The change in mass flow rate, n along the feed side of the membrane area, A is expressed by the total permeation flux, J_p .

$$\frac{dn}{dA} = -J_p \quad (6)$$

The change in composition along the feed side of the membrane may be obtained from a mass balance with respect to the fastest permeating component.

$$\frac{dw}{dA} = \frac{J_p (w-w')}{n} \quad (7)$$

7

With cross-flow on the permeate side of the membrane, the local permeate composition is not affected by the flow pattern (e.g. co-current or counter-current flow), and the composition of the vapor permeating through the membrane may be defined in terms of the membrane selectivity, α .

$$w' = \frac{\alpha w}{1+w(\alpha-1)} \quad (8)$$

If a model is available for calculating α and J_p as a function of the local feed composition w , Eqs. (6)-(8) may be solved numerically. However, an analytical solution may also be obtained provided that suitable assumptions are made with respect to the transport properties α and J_p .

Prediction of the product distribution

The distribution of the components between the two product streams is important in order to evaluate the degree of separation which may be obtained in a given membrane system. By combining the two mass balance equations, a relation between the local feed flow and the local feed composition is obtained.

$$\frac{dn}{dw} = \frac{\frac{dn}{dA}}{\frac{dw}{dA}} = \frac{-n}{w - \alpha w / (1 + w(\alpha - 1))} \quad (9)$$

Eq. (9) is a separable differential equation which may be rearranged into:

$$-\int_{n_f}^{n_p} \frac{dn}{n} = \int_{w_f}^{w_p} \frac{dw}{w - \alpha w / (1 + w(\alpha - 1))} \quad (10)$$

The solution of the left-hand side of Eq. (10) is trivial, and by defining the module cut rate θ as the ratio between permeate flow rate and feed flow rate, the following explicit expression for θ is obtained:

$$\theta = \frac{n_p}{n_f} = 1 - \exp\left(\int_{w_f}^{w_p} \frac{dw}{w - \frac{\alpha w}{1 + w(\alpha - 1)}}\right) \quad (11)$$

The right-hand side of Eq. (11) is still on an integral form, and in order to derive an analytical solution, assumptions regarding membrane selectivity as a function of the local feed composition are needed.

This monotonic behavior suggests that the system performance may be described by a constant average membrane selectivity $\bar{\alpha}$.

$$\bar{\alpha} = \frac{\int_{w_f}^{w_p} \alpha(w) dw}{w_p - w_f} \quad (12)$$

If a linear relation exists between $\ln \alpha$ and the local feed composition w , it may be shown that Eq. (12) is identical to the logarithmic mean membrane selectivity:

$$\bar{\alpha} = \frac{\alpha(w_p) - \alpha(w_f)}{\ln \frac{\alpha(w_p)}{\alpha(w_f)}} \quad (13)$$

With α constant membrane selectivity defined by Eq. (13) an analytical solution of Eq. (11) is obtained.

$$\theta = 1 - \exp\left(\frac{1}{\bar{\alpha}-1}\left(\ln\frac{w_r}{w_f} - \bar{\alpha}\ln\frac{1-w_r}{1-w_f}\right)\right)$$

(14)

Now, the concentration in the permeate stream may be determined from the total mass balance around the membrane module.

$$w_p = \frac{w_f - (1-\theta)w_r}{\theta} \quad (15)$$

This is as expected, since the mass transfer across the membrane surface is analogous to the mass transfer from the liquid to the vapor phase in a differential distillation process, assuming constant membrane selectivity along the membrane surface, and constant relative volatility in the distillation process.

If we consider the retentate stream, the module cut rate θ may be expressed in terms of retentate recovery and retentate purity:

$$\theta = 1 - r_r \left(\frac{1-w_f}{1-w_r}\right) \quad (16)$$

By solving Eq. (14) with respect to the average membrane selectivity, and inserting Eq. (16), we obtain:

$$\bar{\alpha} = \frac{\ln\left(\frac{r_r \frac{1-w_f w_r}{1-w_r w_f}}{r_r \frac{1-w_f w_r}{1-w_r w_f}}\right)}{\ln r_r} \quad (17)$$

A similar expression may be derived with respect to purity and recovery in the permeate stream. In this case the module cut rate is more conveniently expressed in terms of permeate recovery r_p and permeate purity w_p .

$$\theta = r_p \left(\frac{w_f}{w_p} \right) \quad (18)$$

The average membrane selectivity needed to meet a given permeate purity w_p and permeate recovery r_p , using a single membrane stage is given by Eq. (19).

$$\bar{\alpha} = \frac{\ln(1-r_p)}{\ln \left(1 - r_p \frac{1-w_p w_f}{1-w_p w_p} \right)} \quad (19)$$

The membrane area which is required to obtain a specified product purity will have an important impact on the cost of a membrane based separation process. As may be observed from the total mass balance [Eq. (6)], the required membrane area is directly related to the total permeation flux J_p . By rearranging Eq. (6) we may obtain an expression for the required membrane area.

$$A = - \int_{n_f}^{n_r} \frac{dn}{J_p} \quad (20)$$

Therefore we propose to use a constant average permeation flux \bar{J}_p defined as the logarithmic mean between the value of J_p at the feed entrance of the module, and the value of J_p at the retentate exit of the module.

$$\bar{J}_p = \frac{J_p(w_f) - J_p(w_r)}{\ln \frac{J_p(w_f)}{J_p(w_r)}} \quad (21)$$

In this case the following solution of Eq. (20) may be obtained.

$$A = \frac{n_f \theta}{\bar{J}_p}$$

$$A = \frac{n_f \left[1 - \exp \left(\frac{1}{n-1} \left(\ln \frac{w_r}{w_f} - n \ln \frac{1-w_r}{1-w_f} \right) \right) \right]}{\frac{J_p(w_f) - J_p(w_r)}{\ln \frac{J_p(w_f)}{J_p(w_r)}}} \quad (22)$$

The module cut rate may be determined from Eq. (14). Notice that the required membrane area is proportional to the feed flow rate. This is in accordance with the assumptions of plug-flow on the feed-side of the membrane, and negligible pressure drop along the membrane surface.

List of symbols

A membrane area [m²]

w mass fraction of the most permeable

w' mass fraction of the most permeable component on the permeate side

J_p total permeation flux across the membrane [kg.m⁻² h⁻¹]

\bar{J}_p average total permeation flux, Eq. (21) [kg.m⁻² h⁻¹]

n mass flow rate [kg.h⁻¹]

r_p recovery of the fastest permeating component in the permeate stream,

$$r_p = \theta w_p / w_f$$

r_r recovery of the slowest permeating component in the retentate stream,

$$r_r = (1 - \theta) \left(\frac{1 - w_f}{1 - w_f'} \right)$$

α membrane selectivity, $\alpha = w^l/w.h. (1 - w)/(1 - w^l)$ #

$\bar{\alpha}$ average membrane selectivity

θ module cut rate, $\theta = n_p/n_f$

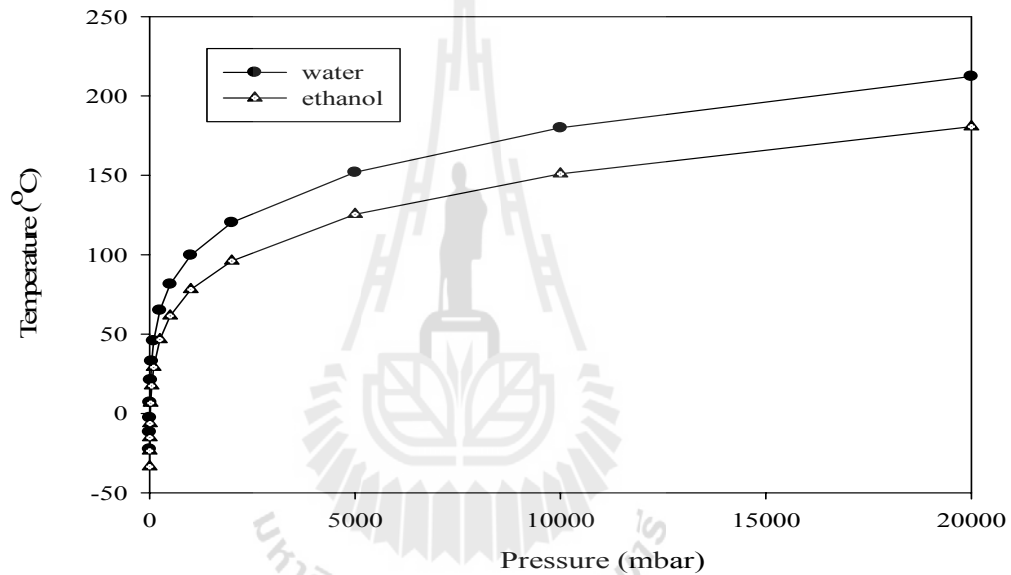


Figure 2.9 Boiling points of water and ethanol at different pressures.

2.3.3 Pressure swing adsorption

Pressure swing adsorption (PSA) is a very versatile technology for separation and purification of gas mixtures. Some of the key industrial applications include gas drying, solvent vapor recovery, fractionation of air, production of

hydrogen from steam methane reformer (SMR) and petroleum refinery offgases, separation of carbon dioxide and methane from landfill gas, carbon monoxide-hydrogen separation, normal isoparaffin separation, and alcohol dehydration. There are several hundred thousand PSA units operating around the world servicing these and other applications (Sircar., 2002).

The PSA process is attractive for the final separation of ethanol from water since it requires little energy input and capable of producing a very pure product. Furthermore, PSA present an easy and quick desorption of the adsorbent only by depressurization (Jianyu Guan and Xijun Hub, 2003). The PSA process rely on the fact that under pressure gases tend to be attracted to solid surface, or adsorbed. The higher the pressure, the more gas is adsorbed; when the pressure is reduced, the gas is released, or desorbed. The PSA processes can be used to separate gases in a mixture because different gases tend to be attracted to different solid surfaces more or less strongly. Aside from their ability to discriminate between different gases and adsorbents for PSA system is usually very porous materials chosen because of their large surface areas. Typical adsorbents are activated carbon, silica gel, alumina and zeolite. The PSA process has proven to be much more energy efficient compared to the classical processes and presently is commercially well established as a separation process for dewatering the mixture of ethanol and water.

The typical PSA cycle includes a production step in which vapor flows into the vessel from the top at a high pressure; water is adsorbed while the ethanol vapor passes through the column and is collected as the high pressure product at the bottom of the bed. After the production step, the bed must be regenerated and prepared for the next cycle. First, the pressure in the bed is reduced while some water

is desorbed. This step is referred as the depressurization step. In the next regeneration step, water is desorbed from the bed under the vacuum. Near the end of the regeneration step, a portion of product gas (99.5% ethanol) is used to purge the vessel to remove the adsorbed water that had been adsorbed during the production step. Then, the vessel is re-pressurized with product ethanol vapor from the operating vessel. The adsorbent bed has then completed its pressure swing cycle and is ready to enter a new production step. Numerous PSA cycles have been devised using two or more adsorbent beds; all of them use the steps described above with slight variations. A precise design of the PSA unit is a difficult task because of many interacting operational parameters characterizing this separation process. Laboratory scale experiments are time consuming and economically demanding. These reasons have lead to the development of mathematical models which are used for initial evaluation of the PSA process. Reliable models enable us to calculate the basic operational characteristics, size the system, and evaluate different scenarios of operation (Simo *et al.*, 2008).

The example of half cycle of ethanol PSA process, sequence of steps and interactions between beds is presented in Figure 2.10. The PSA cycle can be divided into following stages:

(1) Adsorption or production stage. The water–ethanol vapor stream is fed to the bed from the top at 379.2 kPa (55 Psia) and 440K. The high pressure product stream is collected at the bottom of the bed (desirably dry ethanol). A part of the product stream is used to re-pressurize and purge the bed during the desorption stage. The adsorption stage takes about 345 s.

(2) Desorption stage. Following the production stage is completed. The bed must be depressurized, regenerated and repressurized to the adsorption pressure.

1) First depressurization step. Initially, the pressure in the bed is 379.2 kPa and declines to about 137.9 kPa (20 Psia) in 60 s or less. The flow through the valve is critical and the pressure decrease is linear. In our model, the rate of the first depressurization is governed by the cross section of ball valve 1 located on the top of the bed (countercurrent depressurization). The vacuum used during this step is 37.9 kPa (5.5 Psia). For some processes the vacuum used for the first and second steps is the same.

2) Second depressurization step. Pressure at the outlet (top of the bed) is 137.9 kPa and it declines exponentially to 13.8 kPa (2 Psia) in about 150 s. The rate of the second depressurization is governed by the cross section of ball valve 2 located on the top of the bed (counter-current depressurization).

3) Regeneration step with purge. The bed is purged at 13.8 kPa from the bottom of the bed by using a portion of the product stream. This step is very short in the plant; it takes only 15 s.

4) Pressurization. Initially the bed is under the vacuum 13.8 kPa and it is continually pressurized (from the bottom of bed) by the product stream all the way up to 379.2 kPa in about 120 s. The rate of pressurization is governed by the cross section of ball valve 3.

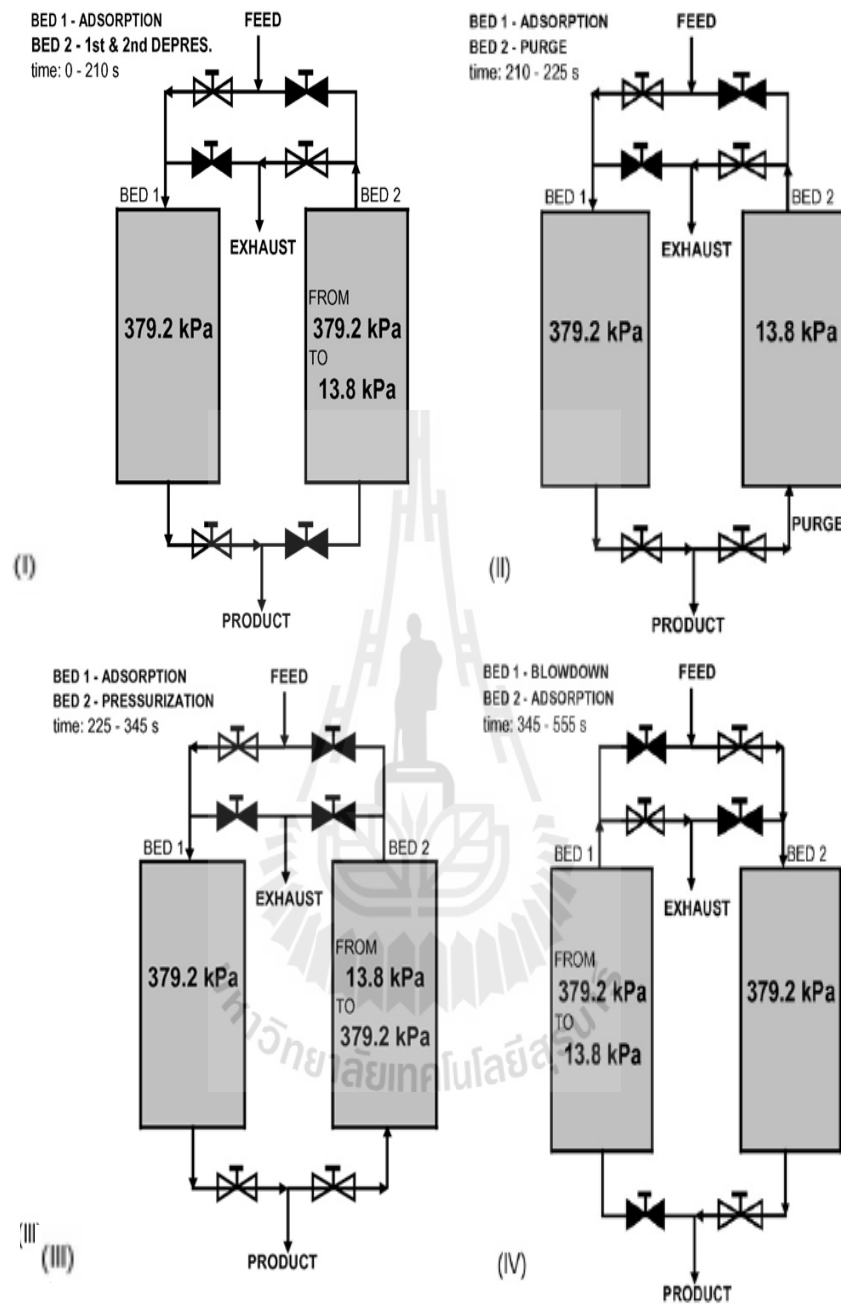


Figure 2.10 Half cycle for ethanol PSA processes (345 s) (steps I.–III.); step IV. represents the switch between the beds (Simo *et al.*, 2008).

The pressure swing adsorption column is filled with beads, with 3 Å micro-pore. Thus, the water molecules are adsorbed while the ethanol molecule are

not. Dehydration by adsorption on a 3- Å molecular sieve has been suggested as a promising alternative to the conventional processes (Hartline, 1979). The 3-A sieve has the advantage that the micropores are too small to be penetrated by alcohol molecules so the water is adsorbed without competition from the liquid phase (Ruthven *et al.*, 1986). Zeolite molecular sieves are adequate adsorbents for the removal of small amounts of water from organic solvents. In virtue of their small diameter (0.28 nm), the water molecules can easily penetrate the structural zeolite canals, while many organic molecules, such as ethanol (0.44 nm), are simultaneously excluded. The Langmuir isotherm satisfactorily correlated the experimental data for the experimental temperatures and concentrations (Carmo *et al.*, 1997). Langmuir isotherm defined by equation 23, which satisfactorily correlated the experimental data.

$$q^* = \frac{Q \cdot K \cdot c^*}{1 + K \cdot c^*} \quad (23)$$

Where c^* is concentration of the liquid phase at equilibrium, weight % water

K is Langmuir's constant, $\text{g}_{\text{sol}}/\text{g}_{\text{water}}$

q^* is concentration of the adsorbed phase at equilibrium, $\text{g}/\text{g}_{\text{ads}}$

Q is Scapacity of the monolayer, $\text{g}/\text{g}_{\text{ads}}$

CHAPTER III

MATERIALS AND METHODS

3.1 Experimental design

This work involved the purification of the ethanol. The ethanol purification process was divided into three steps. From 8-12 to 95 wt% ethanol was obtained using forced-mixing distillation. From 95 to 99 wt% ethanol was obtained using vapor permeation technique. Above 99 wt% ethanol, as the molecular sieve at more than 99.7 wt% ethanol was obtained using pressure swing adsorption technique. The schematic diagram of apparatus for vapor pervaporation and pressure swing adsorption was given below:

มหาวิทยาลัยเทคโนโลยีสุรนารี



Figure 3.1 Setting apparatus of forced-mixing distillation, vapor permeation and pressure swing adsorption: 1, distillation column; 2, condenser; 3, vapor permeation; 4, pressure swing adsorption; 5, feed pump; 6, condenser; 7, oil bath; 8, density meter; 9, refrigerated circulator.

3.2 Materials

3.2.1 forced-mixing distillation: equipment design of forced-mixing distillation column was given as below

1) **Boiler** - To provide the necessary vaporization for the distillation process. The boiler was constructed from stainless steel, 20 cm long and 15 cm in diameter. At the bottom covered by a flat plate (15x15 cm) for placing on the hot plate, at below have a hole for drain the liquid from inside the boiler, beside of boiler had the level indicator. At the top of boiler will be welded by plate flange (18 cm in diameter) and had the hold for setting the other equipments such as gage pressure and gage temperature.

2) **Column** – The column made from a stainless steel, that had 89 cm long and 6.4 cm inner diameter. The top of the column closed by welding with the plate flange (14 cm in diameter) for installation a motor and a drive shaft. At the bottom of column welded the plate flange (14 cm in diameter) with plate flange of boiler. The midpoint of column had a pipe line for the feeding (feeding point), the top of column had a pipe line for releasing the hot vapor (distillate).

3) **Drive shaft** – Drive shaft was the most important part because that used to fix the propellers. The current motor (120 watts) connected directly with the top of a drive shaft by the bolt, which can be adjusted the stirrer speed. Drive shaft had 1.4 cm in diameter and 88.5 cm long. At the top welded closing by plate flange (14 cm in diameter), and had a mechanical seal for high pressure operation (maximum at 6 atm).

4) **Propellers of stripping section** (upflow propellers) - The rising vapors was controlled by propellers of stripping section (upward direction), that composed three-blade paddle mixer with inclined blade (45°) and 1.5 mm thickness. The three-blade paddle was welded with 1.42 cm diameter and 8 mm thickness of a ring. The three-blade paddle had 10 blades, that would have equal space distance installation.

5) **Six-flat blade turbine** - Dispersion increasing of the feed was controlled by six-flat blade turbine, that would set at midpoint of the column.

6) **Propellers of rectifying section** (downflow propellers) - The characteristic of this propellers similarly with the propellers of stripping section but the angle of blade was inclined 135° . The function of this

7) propellers pushed vapors to go down (downward direction) and

descending condensate to the sides of the column cause system accelerated vaporization-condensation cycles along the internal wall of the column which resulted in extremely rapid equilibrium.

3.2.2 Vapor permeation

3.2.2.1 Membrane material

The hydrophilic PVA/PAN-composite membrane supplied by Sulzer Chemtech, Switzerland with a surface area of 0.0288 m^2 ($0.16 \text{ m} \times 0.18 \text{ m}$). A commercial composite membrane prepared from modified Poly(vinyl alcohol) (PVA) as a selective layer and polyacrylonitrile (PAN) as a supportive layer with the membrane thickness of approximately $2 \text{ }\mu\text{m}$, shown in Figure 3.4.

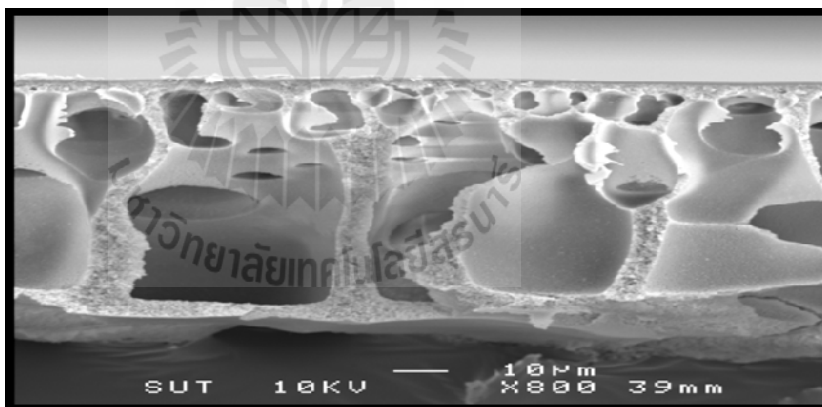


Figure 3.2 SEM images of the composite PVA/PAN membrane.

NaA zeolite hollow fiber which supplied by Mitsui Engineering & shipbuilding, Japan with a surface area of 0.0352 m^2

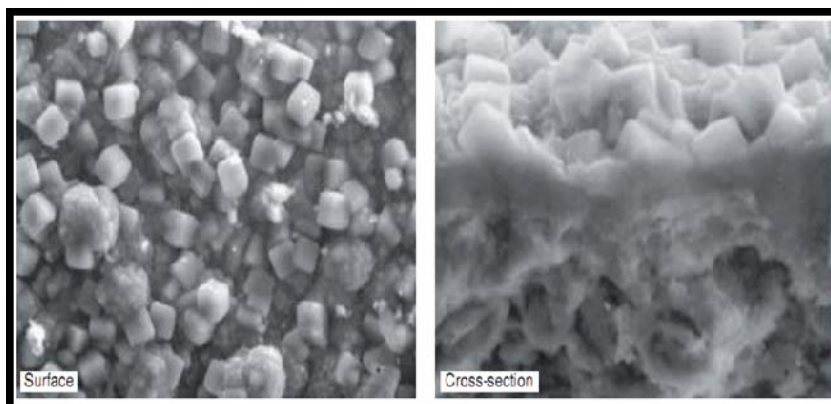


Figure 3.3 Scanning electron microscope photograph of NaA zeolite membrane.



Figure 3.4 NaA zeolite tubular membrane.

3.2.2.2 Commercial grade of ethanol (95% of ethanol)

3.2.2.3 A pressurized vessel

3.2.3 Pressure swing adsorption

3.2.3.1 3-Å molecular sieve



Figure 3.5 Molecular sieves.

3.2.3.2 Adsorption bed, that have 500 ml volume and pack to a height of 30 cm.

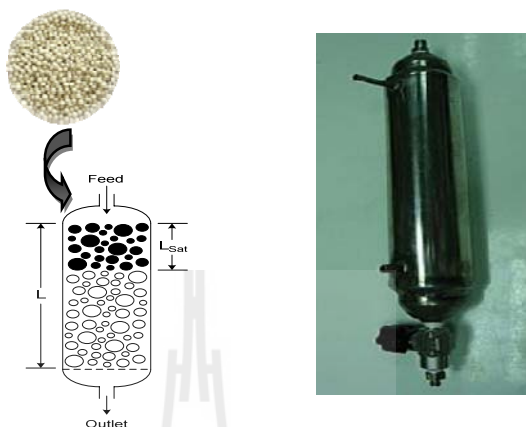


Figure 3.6 Adsorption bed.

3.2.3.3 Commercial grade of ethanol (95% of ethanol)

3.2.3.4 A pressurized vessel

3.2.4 Existing equipments

3.2.4.1 A refrigerated circulator (Julabo, Germany)

3.2.4.2 A vacuum pump (Welch, USA)

3.2.4.3 An on-line density meter (Anton Parr, Austria)

3.2.4.4 An automatic Karl Fischer titrator (Titro Line plus, Schott, Germany)

3.2.4.5 Liquid nitrogen (F1 at Suranaree University of Technology, Thailand)

3.2.4.6 Shell & tube heat exchanger

3.2.4.7 Oil bath (Julabo, Germany)

3.3 Methods

3.3.1 Distillation (forced-mixing distillation)

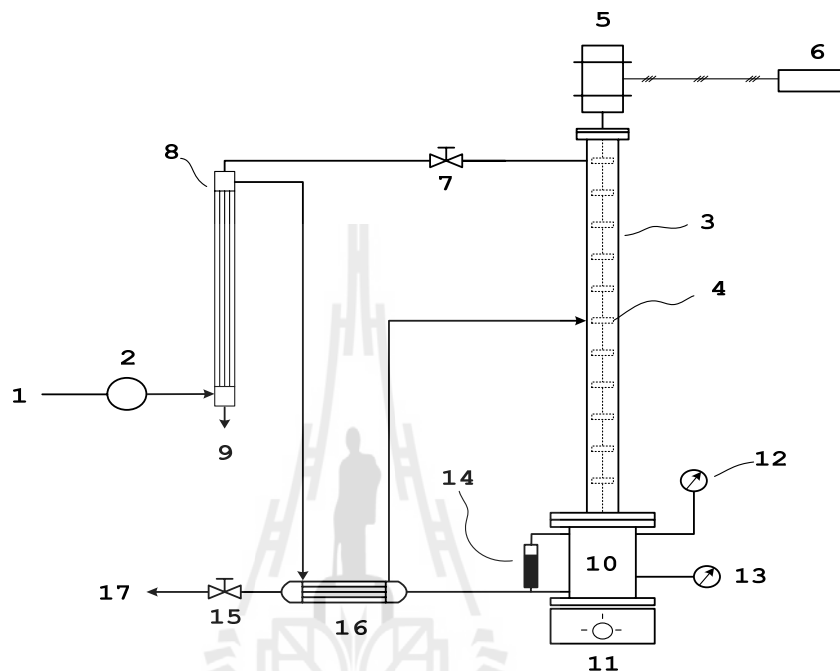


Figure 3.7 Diagram of forced-mixing distillation system.

Figure 3.7 shows the schematic diagram of the patented continuous distillation unit based on forced-mixing concept. The feeding solution (1) was pre-heated by entering the condenser (8), and heat exchanger (16) prior to enter the column through the feeding point located at the middle of the column (4) by pump (2). The column was equipped with a set of internal impellers (3). The middle impeller located at the feeding point served as a dispenser whereas the lower set of impellers had a function of stripping ethanol from fermentation broth. In addition, the

upper set of impellers pushed the rising vapor to partially condense along the side of the column. The high agitation rate resulted in close contact between the vapor and liquid components resulting in a great number of condensation-vaporization cycles. As a result, high efficiency separation was achieved in a short distance of distillation column. At the top of column was connected with motor (5), which can be adjusted the stirrer speed by the controller machine (6). During distillation process, the ethanol vapor was leaved to the top of column by controlling of a ball valve (7) and then ethanol vapor entered to the condenser (8) became to the ethanol-rich product (9). The stillage falled to the boiler (10). A hot plate (11) is used as the main heating device. Inside the boiler had the hold for setting the other equipments such as gage pressure (12), gage temperature (13) and the level indicator (14). This process ran continuously operation so, we was drained the stillage (17) by gage valve (15) passing heat exchanger (16). This system was designed energy saving, that employed 2 heat exchangers to warm the feed solution as well as to cool down the distillate vapor and thin stillage. From Figure 3.9 you can see that feed solution (1) was exchanged heating between with condensed vapor (9) and stillage (17), after that the feed solution (1) had temperature rises up by exchanged heating with condenser (8) and heat exchanger (16). Determination of ethanol concentrations in both feed and product was carried out using Karl Fischer's titration and density meter.

3.3.2 Vapor permeation technique

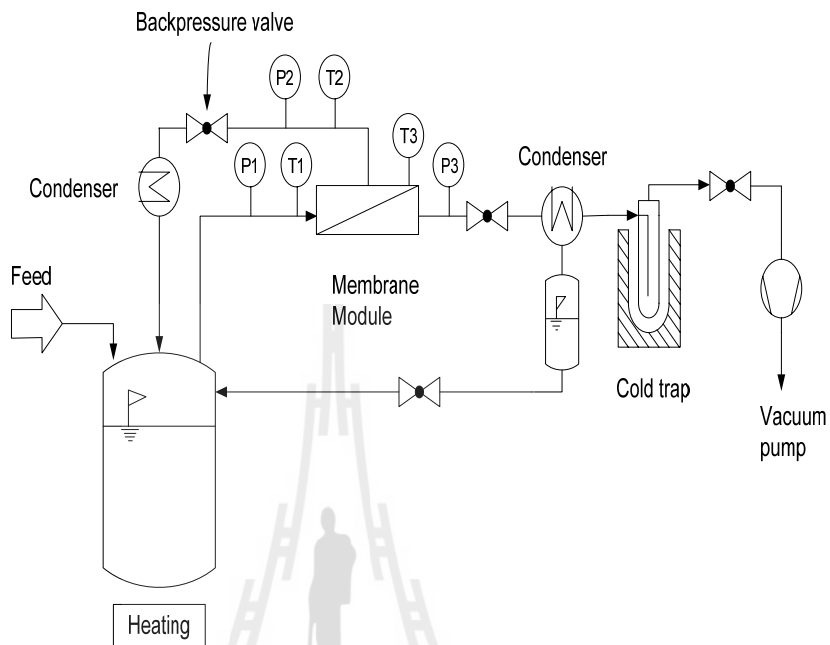


Figure 3.8 Schematic diagram of apparatus for vapor permeation.



Figure 3.9 Membrane module for vapor permeation technique.

Separation experiments for vapor permeation was conducted on a lab scale set up as shown in Figure 3.8. A composite PVA/PAN membrane supplied by

Sulzer Chemtech, Switzerland with a surface area of 0.0288 m^2 ($0.16 \text{ m} \times 0.18 \text{ m}$) was placed in a module, and temperature was controlled by re-circulating silicone oil through jacket surrounding the membrane module. The liquid feed was heated in a pressurized vessel, and the vapor feed then enter the membrane module. The permeate vapor was collected using cold traps immersed in liquid N_2 , and permeate pressure was kept low using a vacuum pump. The permeate was sampled periodically to determine the flux and ethanol composition. The permeation rate was measured gravimetrically by weighing the permeate sample collected over a period of time whilst determination of ethanol concentrations in both feed and permeate were carried out using Karl Fischer's titration and density meter. After that, the type of membrane module we was changed from flat sheet of a composite PVA/PAN membrane to NaA zeolite hollow fiber which supplied by Mitsui Engineering & shipbuilding, Japan.



Figure 3.10 NaA zeolite tubular membrane construct for vapor permeation technique.

3.3.3 Adsorption technique

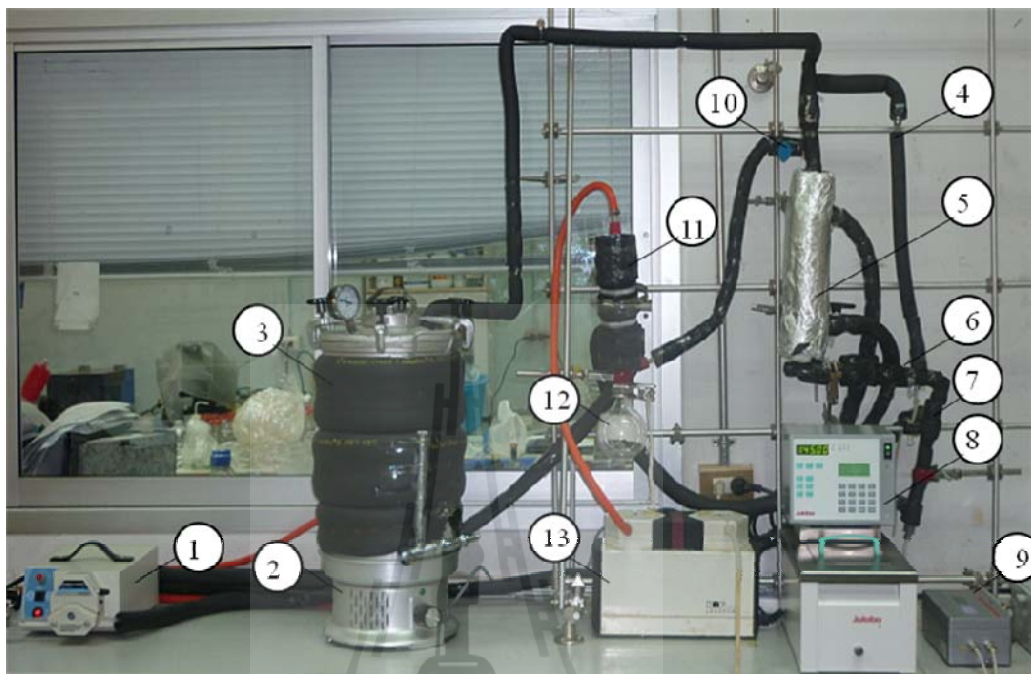


Figure 3.11 Setting of apparatus for adsorption technique: 1, water coolant pump; 2, electrical heater; 3, feed tank; 4, by pass line; 5, adsorption column; 6, samples control valve; 7, heat exchanger; 8, oil bath; 9, density meter; 10, regenerate control valve; 11, condenser; 12, desorbed glass bottle; 13, vacuum pump.

The adsorption experiment apparatus was also conducted as shown in Figure 3.11. The adsorber was made from a stain steel shell with an oil bath jacket surrounded it. The internal volume of the bed was 500 mL which accommodated 386.24 g of molecular sieve beads. The height of the column was 30 cm. Adsorption system using 3-Å molecular sieves was considered. The ethanol- water mixture was stored in a pressurized vessel. The vapor pressure in the column was controlled by

the heater at pressurized vessel. The temperature of the adsorber was well above the dew point of the vapor feed to avoid condensing which the adsorber was heated with 145 °C silicone oil. The vapor feed subsequently went through the column, and the ethanol-rich product was collected at the end of the tube after being condensed. Product samples were collected at every 50 ml and water content was analyzed by Karl Fischer's titrator (Schott, Germany) and density meter to determine the ethanol concentration. When the adsorption reached equilibrium, the experiment passed to regeneration step. The desorbed vapor was collected in a glass bottle that was cooled with water coolant and vacuum pressure.

3.3.4 Hybrid Vapor permeation (NaA zeolite tubular membrane) and Pressure swing adsorption system

The schematic diagram for experimental setup of hybrid VP+PSA system is shown in Figure 3.12. A tubular ceramic membrane supplied by Mitsui Engineering & shipbuilding (Japan) with a surface area of 352 cm² was placed on a module, and temperature was controlled by re-circulating silicone oil through the jacket surrounding it. The liquid feed was heated in a pressurized vessel, and the vapor feed then entered the membrane module. The permeate vapor was collected using a condenser set at -20 °C, and permeate pressure was kept low using a vacuum pump. The permeation rate was measured gravimetrically by weighing the permeate samples collected over a period of time whilst determination of water concentrations in both feed and permeate were carried out using an automatic Karl Fischer's titrator (Schott, Germany). For PSA experiment, two adsorption bed packed with molecular sieve 3Å were used as the final step to dehydrate ethanol vapor with the objective of

the highest purity for up to 99.95 wt%. The individual bed volume was 500 mL, and mass of the molecular sieve was approximately 386 g. The vapor pressure in the column was controlled by a heater of the feed tank. The temperature of the vapor was well above the dew point in order to avoid condensation. The vapor feed subsequently went through the column, and the ethanol-rich product was collected at the end of the tube after being condensed. Product samples were collect at every 50 ml, and water content was analyzed. When the adsorption reached equilibrium, the feed direction was switched to another column where the saturated bed entered regeneration step by applying vacuum. The desorbed vapor was collected in the same permeate glass reservoir as it was used for the VP system. When combining the two processes together, the vapor feed firstly entered the VP module followed by PSA system.

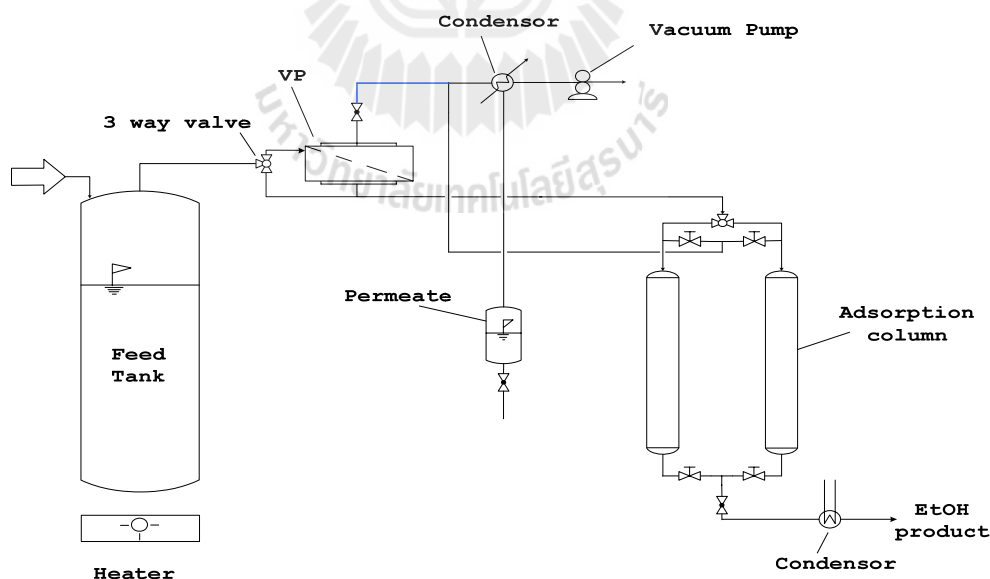


Figure 3.12 Experimental setup for hybrid VP and PSA system.

3.4 Analytical procedures

After we get high purity grade of ethanol we will analyze the product using instrument such as

3.4.1 HYDRANAL® - Moisture Test Kit(Sigma-Aldrich) to determine the water content in samples.

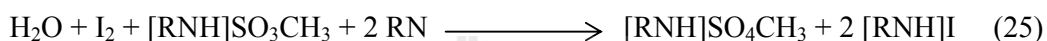
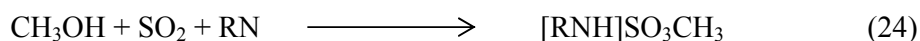


Figure 3.13 Setting of apparatus for an automatic Karl Fisher titration (Titro Line plus, Schott, Germany).

Determination of moisture content in samples using Karl Fischer titration

The determination of water percent in samples is realized through a rapid test kit: HYDRANAL® - Moisture Test Kit (Sigma-Aldrich). The principle applied for the determination of water is based on the Karl Fischer method. It involves the oxidation of sulphur dioxide by iodine with consumption of water. The test kit uses ethanol-based reagents. The solvent, HYDRANAL®-Solvent E, is placed in the

titration vessel and is titrated to dryness using HYDRANAL®-Titrant Component. The end point of the titration is indicated by a sharp colour change from near colourless to yellow. The sample is introduced by means of a syringe, and the titrated again. Karl's Fischer Titration reaction can be defined as follow;



First, the titre of the HYDRANAL®-Titrant component must be determined. The titre is standardized during production, but in case of frequent use of the solution, it is however possible that a drop in titre is brought about by outside influences (introduction of moisture). For this reason it is recommended that a determination of titre is carried out at regular intervals, prior to use.

An exact volume of 0.50 ml of the HYDRANAL®-Standard 5.00 included in the test kit is used in place of the sample. The titre (b) is then calculated from the consumption (a), using the following equation:

$$b = (5.0 * 0.50)/a$$

$$\text{Titre [mg water/mL]}$$

$$= \frac{\text{Water content of standard [mg water/mL]} * \text{Volume of standard [mL]}}{\text{Consumption [mL]}}$$

The water content, in percent by volume, is calculated from the consumption(a), the titre of the titrating solution(b), and the sample volume(V, in µl).

$$c = a * b * 100 / V$$

$$\text{Concentration, in \% by volume} = \frac{\text{Consumption [mL]} * \text{Titre [mg water/mL]} * 100}{\text{Sample volume}[\mu\text{L}]}$$

Remark: The density of ethanol at 20 °C is 0.7893 g.mL⁻¹ and the water density at 20 °C is 0.9982 g.mL⁻¹.

3.4.2 Density meter (Anton Parr, Austria) for determine of ethanol concentrations



Figure 3.14 Density meter (Anton Parr, Austria).

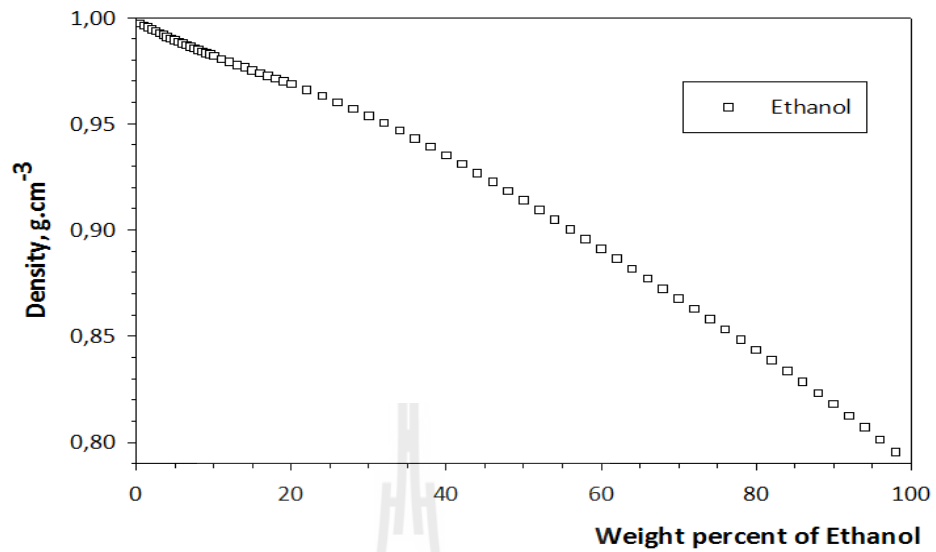


Figure 3.15 Relationship between density and mass fraction of water/ethanol mixture.

3.4.3 Optimization of vapor permeation

The membrane performance can be described by permeate flux J ($\text{kg}\cdot\text{m}^{-2}\cdot\text{h}^{-1}$) and separation factor α defined as follow;

$$J = \frac{W}{At} \quad (2)$$

Where W is the weight of the permeate, A is the membrane area, and t is the time, respectively.

$$J_{\text{water}} = J_{\text{total}} \cdot W_{P,\text{water}} = Q_{\text{water}} \times (p_{\text{water}}^{\text{feed}} - p_{\text{water}}^{\text{permeate}}) \quad (2.1)$$

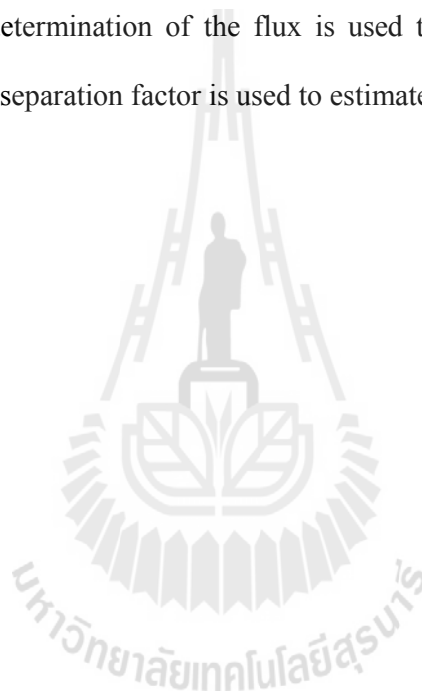
$$J_{\text{ethanol}} = J_{\text{total}} \cdot W_{P,\text{ethanol}} = Q_{\text{ethanol}} \times (p_{\text{ethanol}}^{\text{feed}} - p_{\text{ethanol}}^{\text{permeate}}) \quad (2.2)$$

Where Q is the permeance ($\text{mol.m}^{-2}.\text{s}^{-1}.\text{Pa}^{-1}$)

$$\alpha = \frac{w_{P,\text{water}}/w_{f,\text{water}}}{w_{P,\text{ethanol}}/w_{f,\text{ethanol}}} \quad (3)$$

Where w_f and w_P are the weight fraction of water and ethanol in the feed and permeate side respectively.

The determination of the flux is used to estimate the productivity of separation, and the separation factor is used to estimate the method efficiency.



CHAPTER IV

RESULTS AND DISCUSSIONS

4.1 Forced-mixing distillation

The influence of stirrer speed on distilled ethanol concentration at different feed flow rates from 12 wt% feed ethanol concentration was illustrated in Figure 4.1. The experiments were operated in continuous mode. From the results, the purity of ethanol was a function of stirrer speed, and feed flow rate. It can be seen that, ethanol concentration in the product stream increased with increasing feed flow rate from 1.4 to 3.2 mL.min⁻¹ and the optimum stirrer speed was about 1,000 rpm which achieved highest produced 95 wt% ethanol.

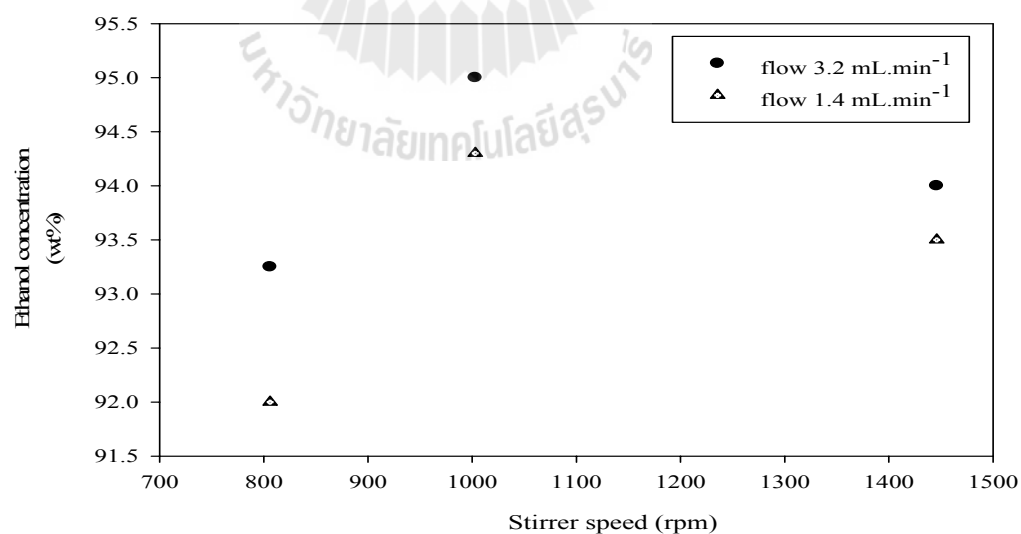


Figure 4.1 The relationship between stirrer speed and ethanol concentration at different feed flow rates; feed 12 wt% ethanol.

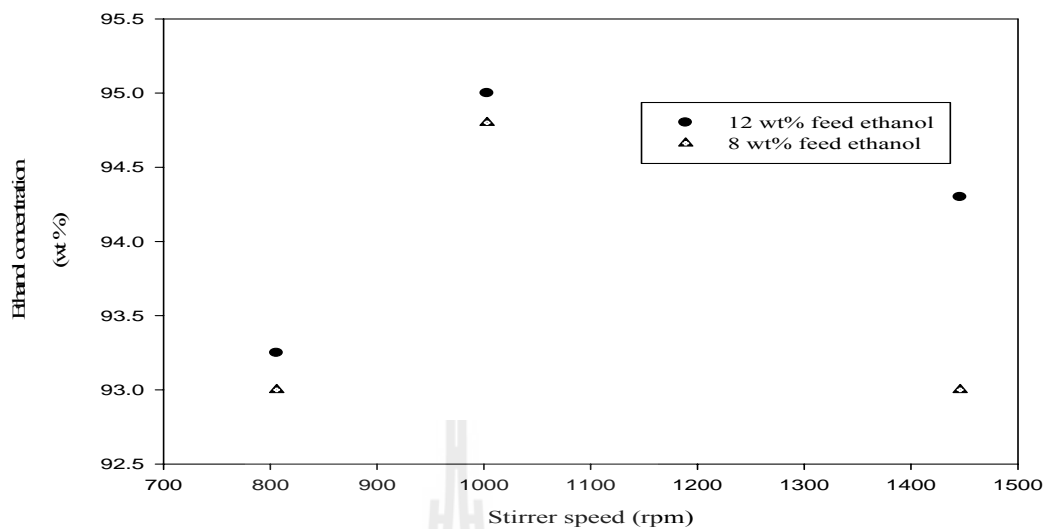


Figure 4.2 The relationship between stirrer speed and ethanol concentration at difference feed compositions; flow rate $3.2 \text{ mL}\cdot\text{min}^{-1}$.

The influence of stirrer speed on ethanol concentration at different feed compositions was illustrated in Figure 4.2. Experimental results revealed that the purity of ethanol was a function of stirrer speed and feed composition. It can be seen that, at the optimum stirrer speed of approximately 1,000 rpm, the system can produce 95 wt% of ethanol, and the purity of ethanol increased with increasing ethanol concentration from 8 wt% to 12 wt%. The highest ethanol concentration was obtained at approximately 95 wt% for distillation which is the same quality as industrial scale distillation. From both Figures, it was obviously shown that stirrer speed of 1,000 rpm resulted in the highest purity of ethanol in the distillate. Therefore, this rotational speed was employed for the rest of the experiment.

In addition, the experimental VLE data for the ethanol–water binary system were shown in Figure 4.3 as an x - y diagram. Two distinct experiments were carried

out by using simple distillation, and our distillation system. The main objective for investigating the VLE of the first system was first to check for the practical feasibility of our novel distillation unit using the forced-mixing concept, and to compare distillation performance of the two systems. Experimental results for simple distillation showed a very good agreement with the UNIQUAC, and Antoine's correlation. In comparison with our distillation unit, the VLE diagram has been altered reaching the azeotropic point at the mass fraction of ethanol in the liquid phase ($x_{ethanol}$) as low as 0.05. Even $x_{ethanol}$ of 0.04, the ethanol mass fraction in the vapor phase ($y_{ethanol}$) was 0.88. This particular system would support other research works of ethanol production especially cellulosic substrates where final concentration of ethanol in the fermentation broth was relatively low. In addition, these excellent experimental results of VLE data could pave a way to develop the new concept of distillation to replace the existing fractionating column. For an industrial scale, the column internal might possess more than 70 active plates resulting in high investment cost and high energy input for distillation. It is the fact that distillation of ethanol was only achieved in an industrial scale making the small scale production of fuel grade ethanol very difficult. The alteration of the VLE using forced-mixing concept was due to the effect of an extremely high number of the vaporization-condensation cycle on the mixture components. This effect was also a function of the homogeneity of the raising vapor inside the column. This distillation system was also designed for the continuous mode. The demand of energy input was expected at the lowest because the feed was used as the coolant for both distillate and thin stillage. The feed was also pre-heated almost to its boiling point before entering the column, thus substantially lowered the heat demand.

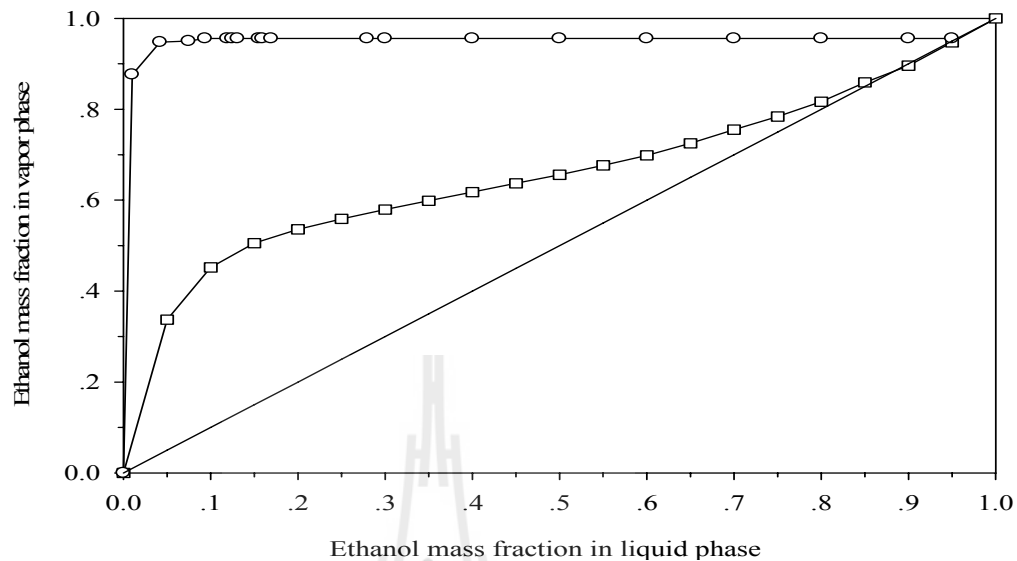


Figure 4.3 Experimental vapor-liquid equilibrium data for ethanol/water binary system; straight line (-) was 45° line, the open square (□) was the data obtained from simple distillation whilst the curve was generated from equation (1), open circle (○) was the data obtained from our distillation system.

4.2 Vapor permeation

4.2.1 The hydrophilic PVA/PAN-composite membrane

Application of the composite PVA/PAN membrane from Sulzer Chemtech, Switzerland for dehydration of ethanol was investigated using vapor permeation technique at operating pressure between 1.2-1.8 bars, and module temperature between 80-120 °C. Higher module temperature was not investigated because this value was the maximum temperature recommended by the manufacturer. The retentate (product) flow was controlled by a back pressure valve with the flow

rates between 0.875-3.025 mL.min⁻¹. Separation of water and ethanol is governed by preferential absorption into the cross-linked polymer, and mass transfer characteristic is also affected by operating conditions. In this work, separation performances were investigated including the effect of feed ethanol mass fractions, retentate flow rate, feed pressures, and operating temperatures, respectively.

4.2.1.1 Effect of feed pressure

The influence of feed pressure on ethanol concentration in the retentate was illustrated in Figure 4.4. It was shown that the ethanol concentration strongly depended on the feed pressure indicating that the higher quality ethanol concentration in retentate can be achieved at higher feed pressure. The ethanol concentration increased from 96.82 to 98.86 wt% as the feed gage pressure increased from 1.2 to 1.8 bars.

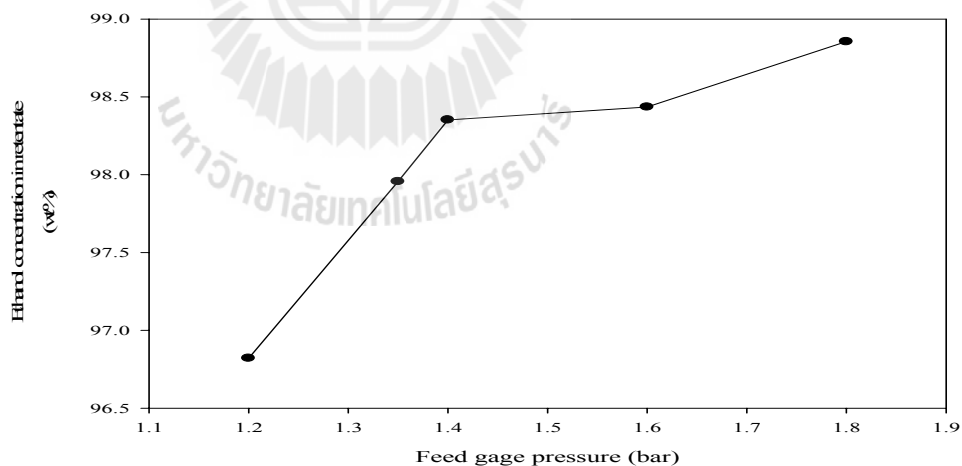


Figure 4.4 The compositional evolution in ethanol retentate with proceeding of dehydration at different feed pressures; flow rate 1.85 mL.min⁻¹, feed concentration of ethanol 95 wt% and cell temperature of 120 °C.

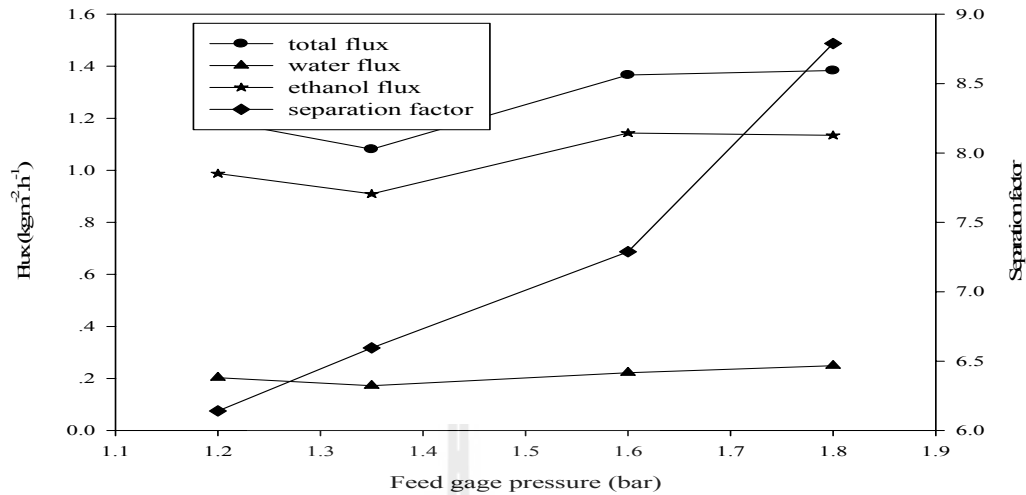


Figure 4.5 The influence of operating feed gage pressure on fluxes and separation factor with 95 wt% of ethanol in the feed side, vacuum 6 mbar, retentate flow rate 1.85 mL.min⁻¹, and cell temperature of 120 °C.

In this experiment, permeation experiments were carried out at different feed gage pressure, and separation performances were investigated in terms of fluxes and separation factor. Figure 4.5 showed the effect of operating feed gage pressure on total flux, ethanol flux, water flux, and separation factor, respectively. For separation factor, it was clearly seen that separation factor significantly increased with increasing feed pressure. The separation factor increased from 6.14 to 8.79 as the feed gage pressure increased from 1.2 to 1.8 bars. However, there was no specific tendency in fluxes for total, ethanol, and water. Total flux slightly increased from 1.21 to approximately 1.40 kg.m⁻².h⁻¹ whereas ethanol flux remained constant at 0.2 kg.m⁻².h⁻¹ throughout the experiments.

4.2.1.2 Effect of cell temperature

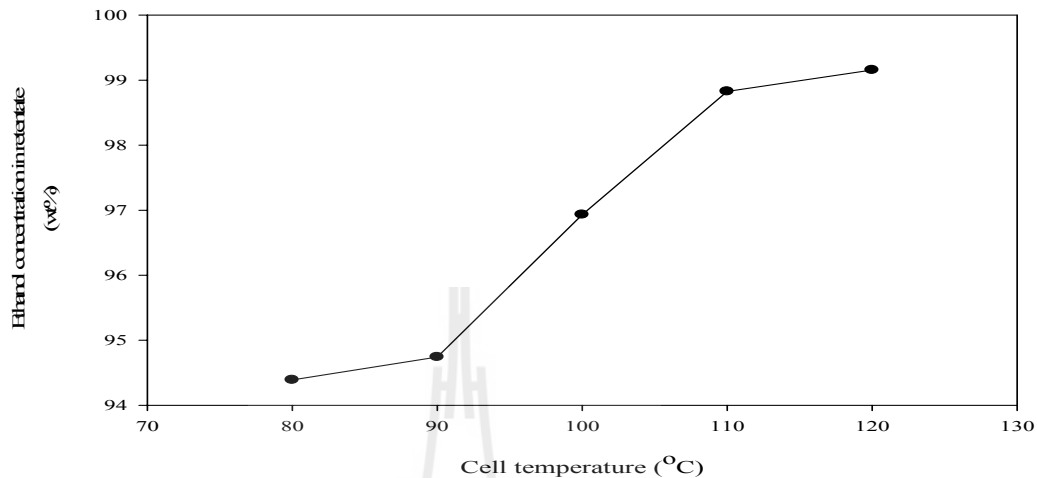


Figure 4.6 The effect of module temperature on the purity of ethanol in the retentate stream; feed pressure gage 1.4 bars, feed concentration 95 wt% and flow rate $0.95 \text{ mL}\cdot\text{min}^{-1}$.

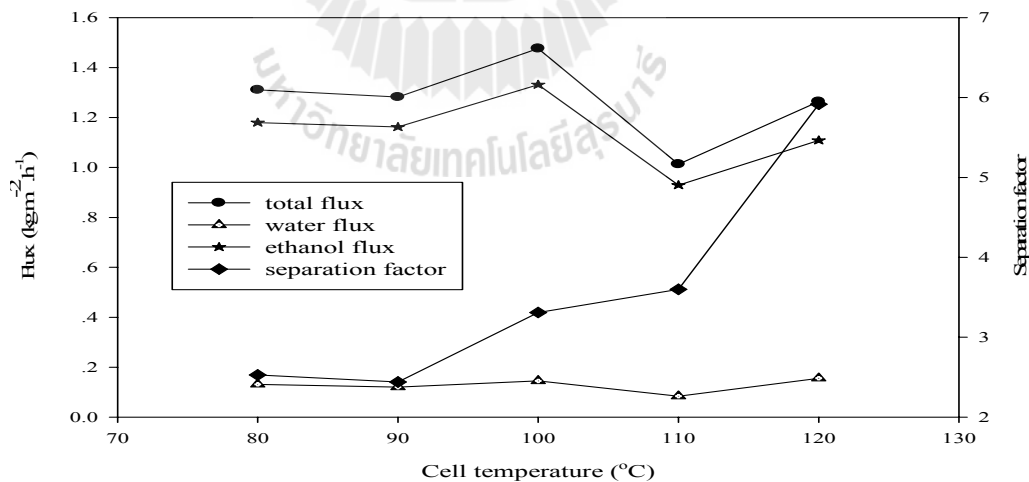


Figure 4.7 The influence of operating module temperature on fluxes and separation factor with 95 wt% of ethanol in the feed side, vacuum 6 mbar, feed gage pressure 1.4 bars and retentate flow rate $0.95 \text{ mL}\cdot\text{min}^{-1}$.

The effect of operating module temperature on ethanol concentration in the retentate stream was shown in Figure 4.6. The experimental results show that the ethanol concentration in the product was strongly depended on the module temperature, indicating that the higher quality ethanol concentration in retentate can be achieved at higher module temperature.

Figure 4.7 demonstrated a membrane performance with various module temperatures during vapor permeation of an ethanol-water mixture through a composite PVA/PAN membrane. The ethanol content in feed was 95 wt%, vacuum 6 mbar, feed gage pressure 1.4 bars, and retentat flow rate $0.95 \text{ mL}\cdot\text{min}^{-1}$, respectively. Usually, when the temperature of the module was higher, the diffusivity of permeant molecules will be increased, but the activity of feed vapor was reduced resulting in a significant decline in the solubility of the vapor in the membrane (C.K. Yeom and K.-H.,Lee, 1997). Separation factor was observed to slightly change with increasing of module temperature from 80 to 100 °C, but dramatically change with increasing of cell temperature from 110 to 120 °C. It might be explained that higher module temperature could produce a higher saturated vapor pressure which would increase the solubility of feed vapor into the membrane, and thus the difference in densities of the saturated vapor or the interfacial resistance could be lowered to increase a net flux across the interface between feed and membrane. In addition, high module temperature could also be positive factor for the vapor permeation of ethanol-water mixtures (C.K. Yeom and K.-H.,Lee, 1997).

4.2.1.3 Effect of retentate flow rate

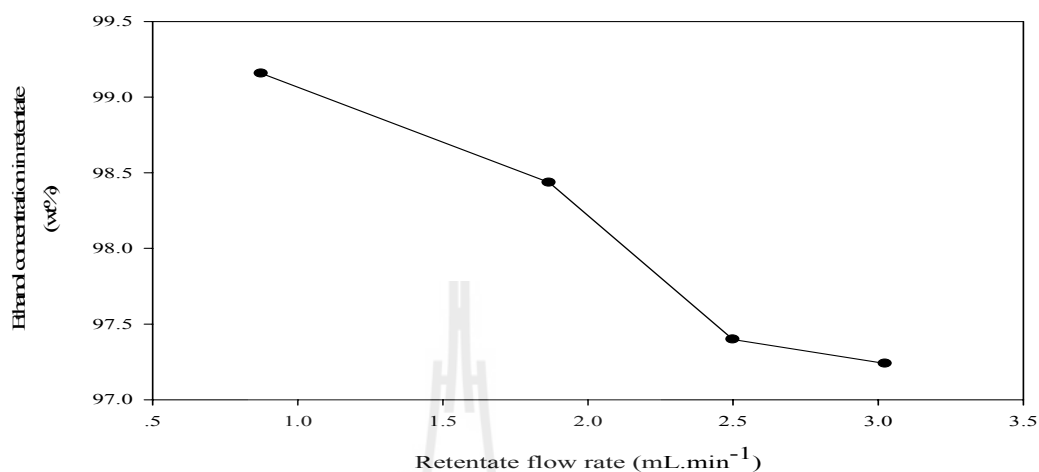


Figure 4.8 The compositional evolution in ethanol retentate with proceeding of dehydrating at different retentate flow rate; feed pressure gage 1.6 bars, feed concentration of ethanol 95 wt% and cell temperature of 120 °C.

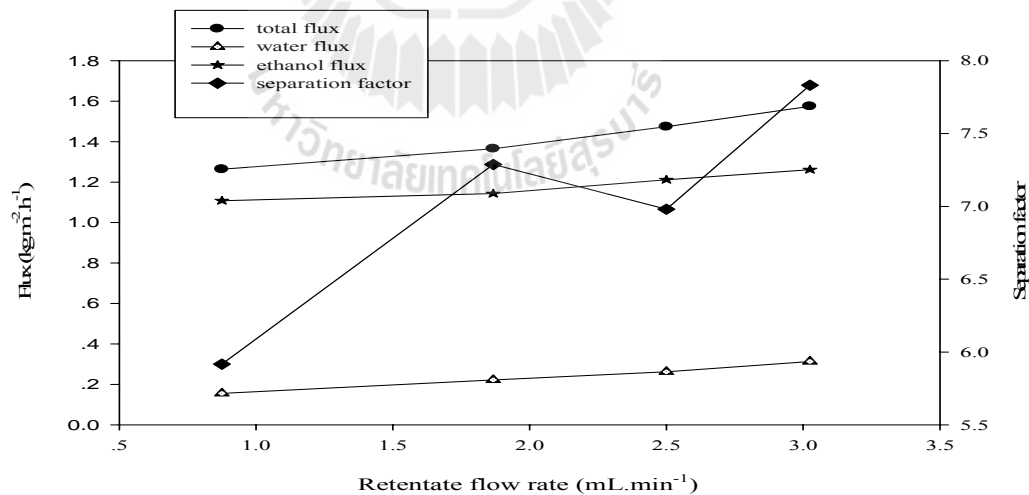


Figure 4.9 The influence of retentate flow rate on fluxes and separation factor with 95 wt% of ethanol in the feed side, vacuum 6 mbar, feed gage pressure 1.6 bars and cell temperature of 120 °C.

The effect of operating retentate flow rate on ethanol concentration in the retentate was shown in Figure 4.8. The experimental results showed that the ethanol concentration was depended on the retentate flow rate indicating that the higher purity of ethanol in the retentate stream could be obtained at lower flow rate. This reason is water vapor was continuously removed along its flow path.

The influence of retentate flow rate on fluxes and separation factors were illustrated in Figure 4.9. It was shown that total, ethanol, and water fluxes increased with increasing retentate flow rate. The total fluxes increased from 1.26 to 1.57 $\text{kg}\cdot\text{m}^{-2}\cdot\text{h}^{-1}$ as the retentate flow rate increased from 0.88 to 3.03 $\text{mL}\cdot\text{min}^{-1}$. For ethanol and water, it was clearly shown that water fluxes and ethanol fluxes were slightly increased with increasing of retentate flow rate. For separation factor, it was clearly seen that separation factor dramatically increased with the increasing retentate flow rate.

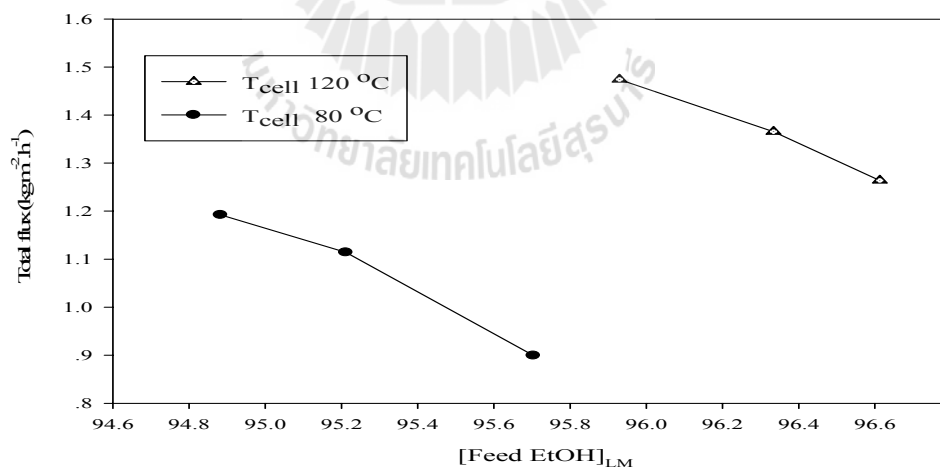


Figure 4.10 Effects of feed compositions on total fluxes; 6 mbar vacuum pressure.

The effect of initial feed ethanol concentration at various module temperatures on total flux was shown in Figure 4.10. The experimental results showed that the total fluxes increased with increasing feed water content, and also increasing of module temperature. The effect of concentration polarization in vapor permeation had already been investigated in detail, and had been found to be of minor importance for the PVA/PAN-composite membrane. Due to the fact that in a vaporous phase diffusivities were about three to five orders of magnitude larger than in a liquid phase, it was expected that concentration polarization in vapor permeation in general was smaller than in pervaporation. However, as the density in a vapor was about three orders of magnitude smaller than in liquid, the increase in mass transport to the feed side boundary of the membrane caused by the larger diffusivities was partly compensated. Nevertheless, the larger diffusivities in vapor permeation favored diffusive back-mixing and, therefore, the effect of concentration polarization in vapor permeation was not as significant as in pervaporation (R. Rautenbach and F.P. Helmus, 1994). As a consequence, the different separation behavior of the PVA/PAN-composite membrane in vapor permeation cannot be caused by concentration polarization (M.S. Schehlmann *et al.*, 1995).

In conclusion, the highest purity ethanol concentration of 99.16 wt% was obtained from this experiment with the following operating conditions: temperature of module 120 °C, retentate flow rate 0.875 mL.min⁻¹, and feed pressure gage of 1.6 bars. However, higher concentration of ethanol could not be achieved, and this was because separation become more difficult at very high ethanol concentration due to low driving force.

4.2.2 NaA zeolite hollow fiber

For comparison purpose, an application of the NaA zeolite tubular membrane supplied by Mitsui Engineering & shipbuilding, Japan with a surface area of 0.0352 m² was also investigated using vapor permeation technique. The system performance was investigated at operating pressure between 0.4-3 bars, and module temperatures between 110-145 °C. Because the membrane was fabricated from ceramic material, it exhibited higher mechanical and thermal stability than polymeric membrane. The retentate (product) flow was also controlled by a back pressure valve with the flow rates between 5.17-21.83 mL.min⁻¹. Separation of water and ethanol was governed by molecular sieve property of the zeolite, and mass transfer characteristic was also affected by operating conditions.

4.2.2.1 Effect of feed pressure

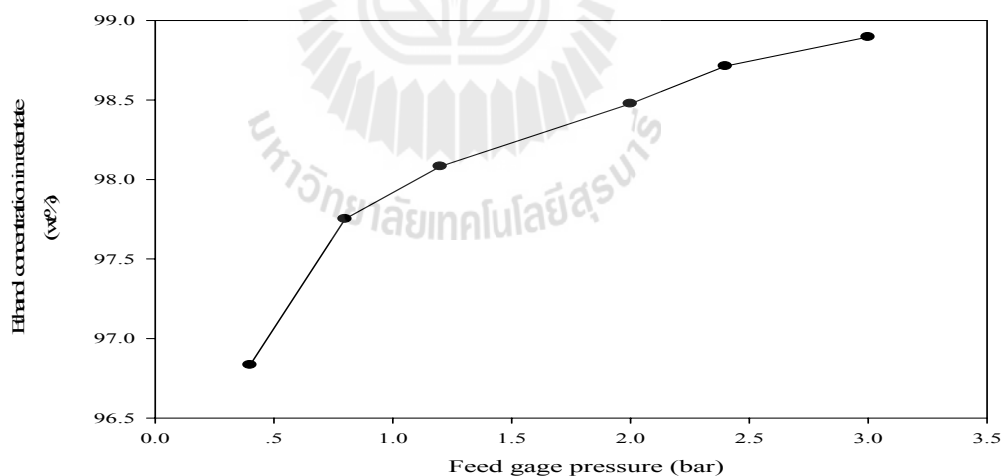


Figure 4.11 The effect of feed gage pressure on ethanol purity in the retentate; flow rate 7.8 mL.min⁻¹, cell temperature of 145 °C, feed concentration of ethanol 95 wt%, and vacuum pressure 6 mbar.

The influence of feed pressure on ethanol concentration in the retentate stream using NaA zeolite tubular membrane was illustrated in Figure 4.11. It was shown that the ethanol concentration was also depended on the feed pressure indicating that the higher quality ethanol concentration in retentate could be achieved at higher feed pressure. The ethanol concentration increased from 96.83 to 98.90 wt% as the feed gage pressure increased from 0.4 to 3 bars. In general, ceramic membrane revealed better dehydration performance compared to polymeric membrane. Water fluxes and separation factor were relatively higher due to molecular sieve characteristic of the zeolite used. The pressure was able to be operated for up to 3.0 bars. Therefore the ceramic membrane was the membrane of choice for hybrid dehydration system.

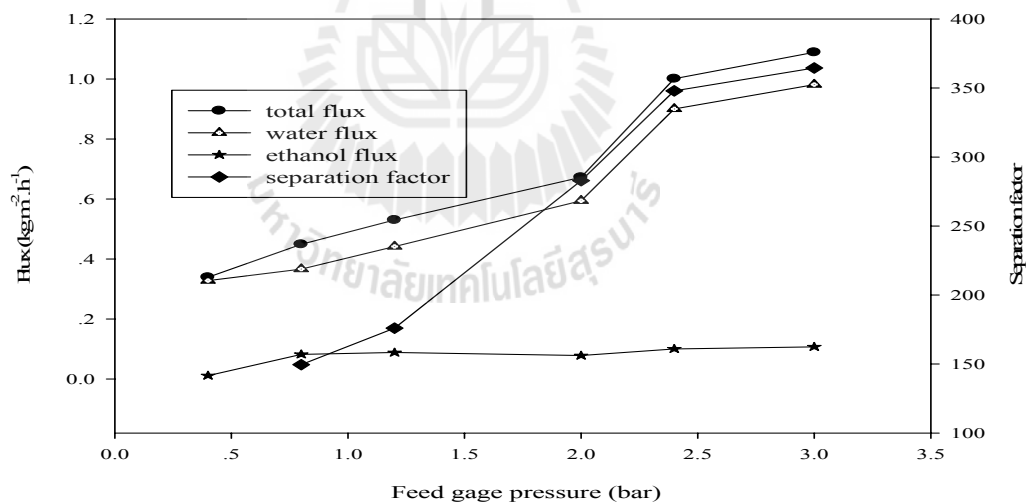


Figure 4.12 The influence of operating feed gage pressure on fluxes and separation factor with 95 wt% of ethanol in the feed side, vacuum 6 mbar, retentate flow rate about 7.8 mL.min⁻¹, and cell temperature of 145 °C.

Figure 4.12 shows the effect of operating feed gage pressure on fluxes and separation performances of NaA zeolite hollow fiber. Permeation experiments

were carried out at different feed gage pressure, and membrane performances were also investigated in terms of fluxes and separation factor. Total flux, and water flux, increased with an increasing operating feed pressure indicating that the membrane would work much better at higher operating feed pressure. In addition, ethanol flux remained close to zero throughout the testing conditions. For separation factor, it was clearly seen that separation factor increased rapidly with increasing feed pressure. The separation factor increased from 149.55 to 364.55 as the feed gage pressure increased from 0.8 to 3.0 bars.

4.2.2.2 Effect of cell temperature

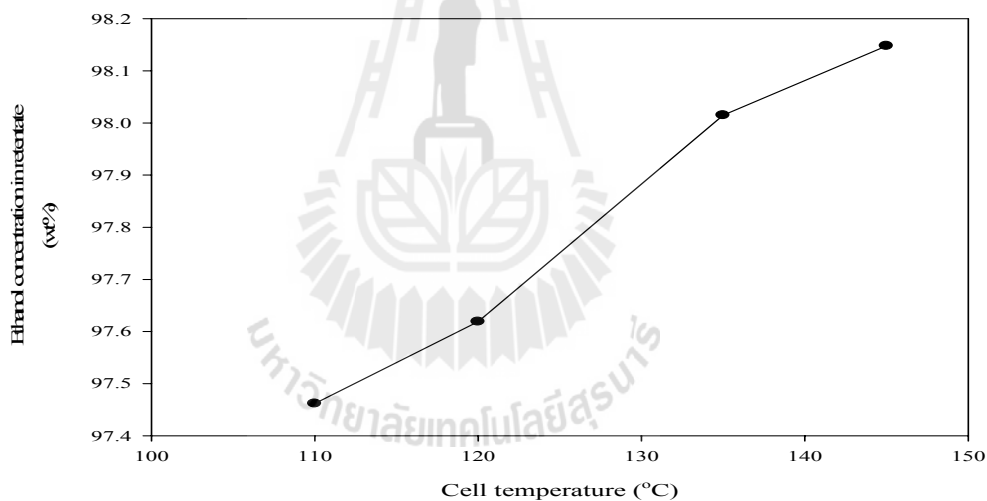


Figure 4.13 The compositional evolution in ethanol retentate with proceeding of dehydrating at different cell temperature; feed pressure gage 1.6 bars, feed concentration of ethanol 95 wt%, and 6 mbar vacuum pressure.

The effect of operating module temperature on ethanol concentration in the retentate stream of NaA zeolite membrane was shown in Figure 4.13. The experimental results showed that the ethanol concentration was depended on the

module temperature, indicating that the higher quality ethanol concentration in retentate could be obtained at higher module temperature. The ethanol concentration increased from 97.46 to 98.15 wt% as the cell temperature increased from 110 to 145 °C.

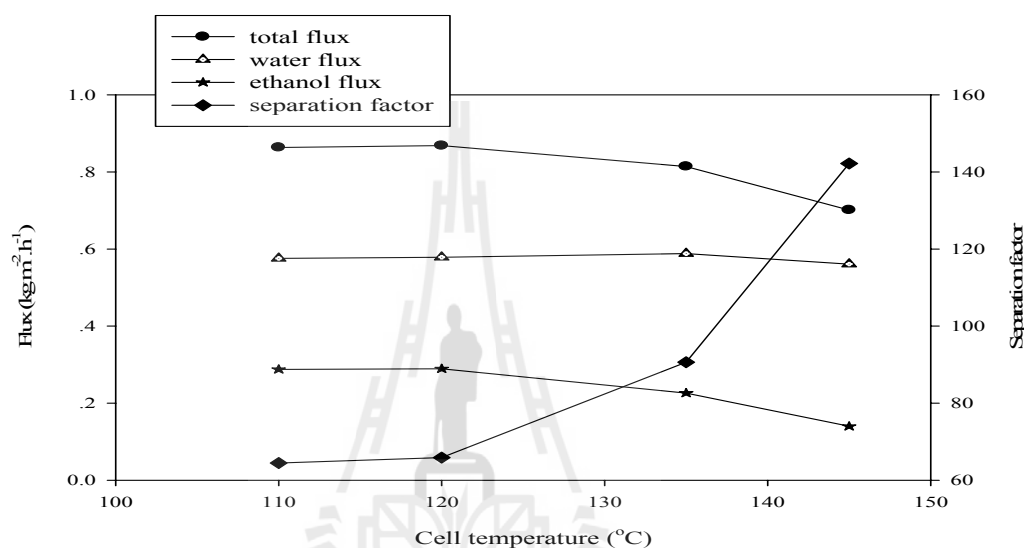


Figure 4.14 The influence of operating cell temperature on fluxes and separation factor with 95 wt% of ethanol in the feed side, vacuum 6 mbar, feed gage pressure 1.6 bars, and retentat flow rate 0.95 mL.min⁻¹.

The membrane performance of permeation fluxes and separation factors (α) through the synthesized NaA zeolite membrane with asymmetric support were examined in a mixture of water (5 wt%)/ethanol (95 wt%) at 110–145 °C and they were shown in Figure 4.14. For total flux and ethanol flux, it was clearly seen that total flux and ethanol flux decreased slightly with increasing cell temperature. These results clearly indicated that the dehydration through NaA zeolite membranes was thermally activated process and the increased of temperature enhanced water flux to increase very slightly. For separation factor, it was clearly seen that separation factor

increased rapidly with increasing cell temperature from 120 to 145 °C. Therefore, the operating condition at higher temperature and pressure were beneficial to exploit the properties of the NaA zeolite membrane for high performance in dehydration process. Although we did not have the experimental data of heat adsorption of water to NaA zeolite at higher temperatures up to 145 °C, it was reported that the adsorption amount of water to NaA zeolite was decreased with increasing temperature (D.W. Breck, 1974). So this might be implied that the higher temperature conditions could alter adsorption behavior accompanying with decreasing values of heat adsorption. Therefore, the observed significant negative temperature dependency of water permeance through NaA zeolite membrane could be occurred at higher temperatures at 100-145 °C by the temperature influenced on the adsorption and diffusion properties (Sato *et al.*, 2007).

4.2.2.3 Effect of retentate flow rate

The effect of operating retentate flow rates on ethanol concentration in retentate of NaA zeolite tubular membrane was shown in Figure 4.15. The experimental results showed that the ethanol concentration was depended on the retentate flow rate indicating that the higher quality retentate could be obtained at lower flow rate.

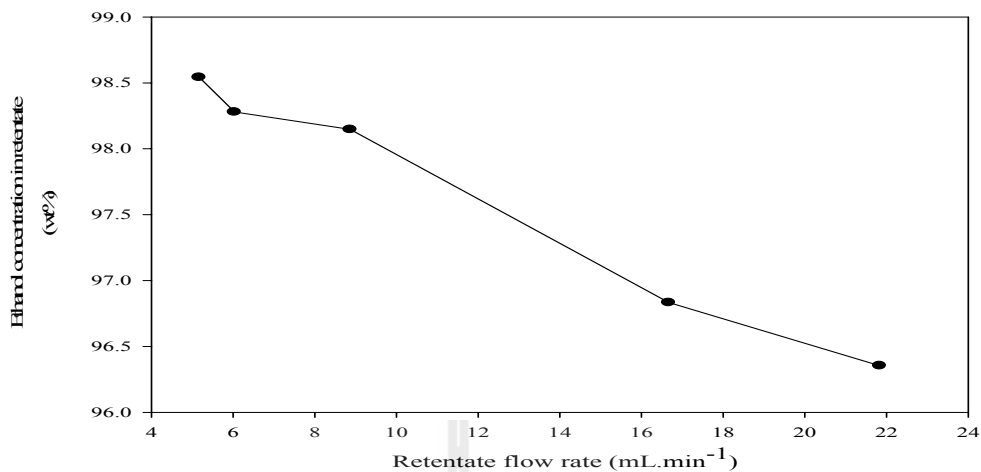


Figure 4.15 The compositional evolution in ethanol retentate with proceeding of dehydrating at different retentate flow rates; feed pressure gage 1.6 bars, feed concentration of ethanol 95 wt%, 6 mbar vacuum pressure and cell temperature 145 °C.

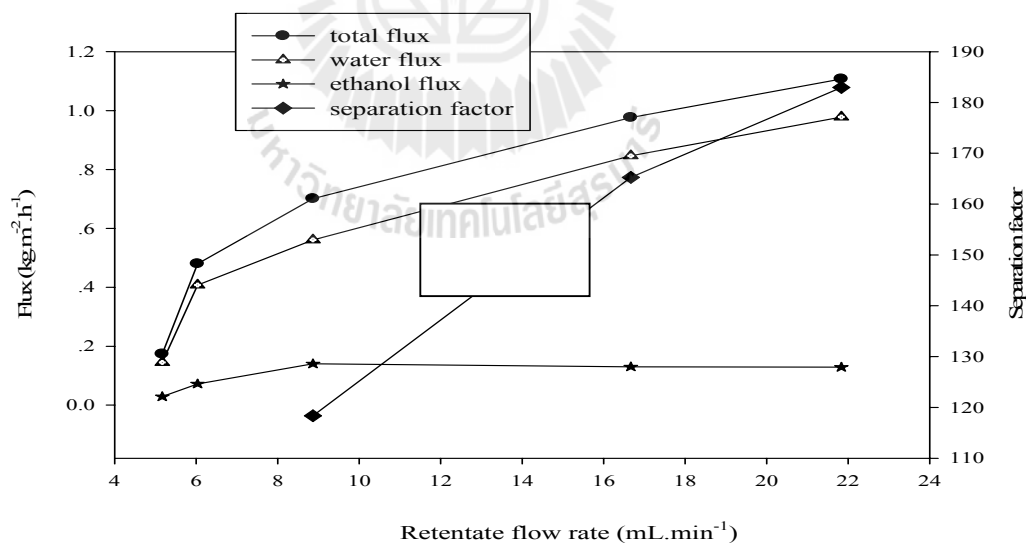


Figure 4.16 The influence of operating retentates flow rate on fluxes and separation factor with 95 wt% of ethanol in the feed side, vacuum 6 mbar, feed gage pressure 1.6 bars and cell temperature 145 °C.

The influence of retentate flow rate on fluxes and separation factors factor with 95 wt% of ethanol in the feed side, vacuum 6 mbar, feed gage pressure 1.6 bars and cell temperature 145 °C were illustrated in Figure 4.16. The experimental results showed that, the total flux, ethanol flux, and water flux increased slightly with increasing retentate flow rates from 5.17 to 21.83 mL.min⁻¹. For separation factor, there was no specific tendency in separation factor with increasing retentate flow rates from 5.17 to 8.87 mL.min⁻¹, but separation factor increased rapidly from 142.18 to 212.13 with increasing the retentate flow rates from 8.87 to 21.83 mL.min⁻¹.

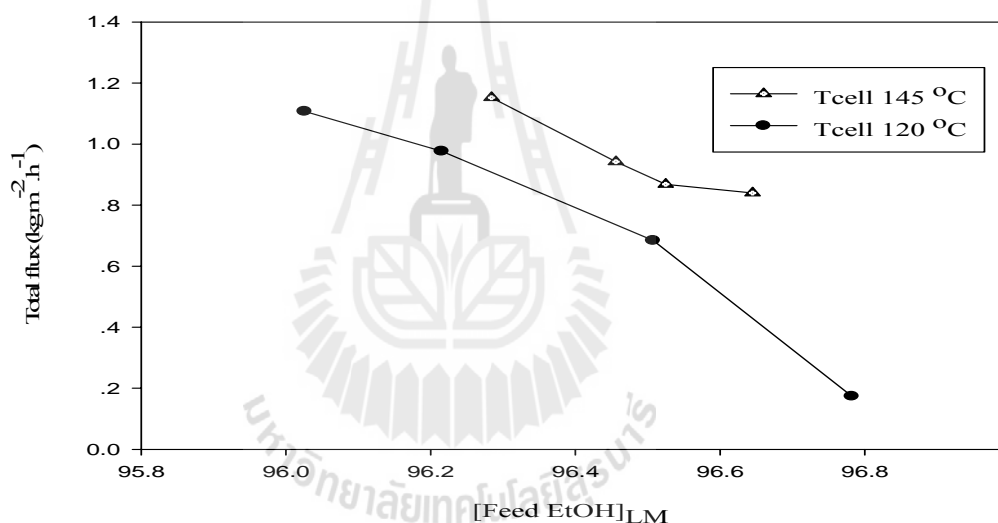


Figure 4.17 Effects of feed compositions on total fluxes, 6 mbar vacuum pressure.

The effect of module temperature and initial feed ethanol concentration on total flux of NaA zeolite tubular membrane was shown in Figure 4.17. The experimental results showed that the total fluxes increased with increasing feed water content as well as module temperature.

The relationship between the permeation flux and the feed temperature

provide important information on the permeating properties, because the temperature is one of the most important operating parameter for the engineering design in dehydrating process. It was noted that temperature influences three important properties (i) adsorption, (ii) diffusion and (iii) vapor pressure in the feed during the permeation through zeolite membrane. The third parameter of the vapor pressure in the feed was the driving force for the permeation flux through the zeolite membrane (Sato *et al.*, 2007).

4.2.3 Mathematical simulation of required purity on membrane area

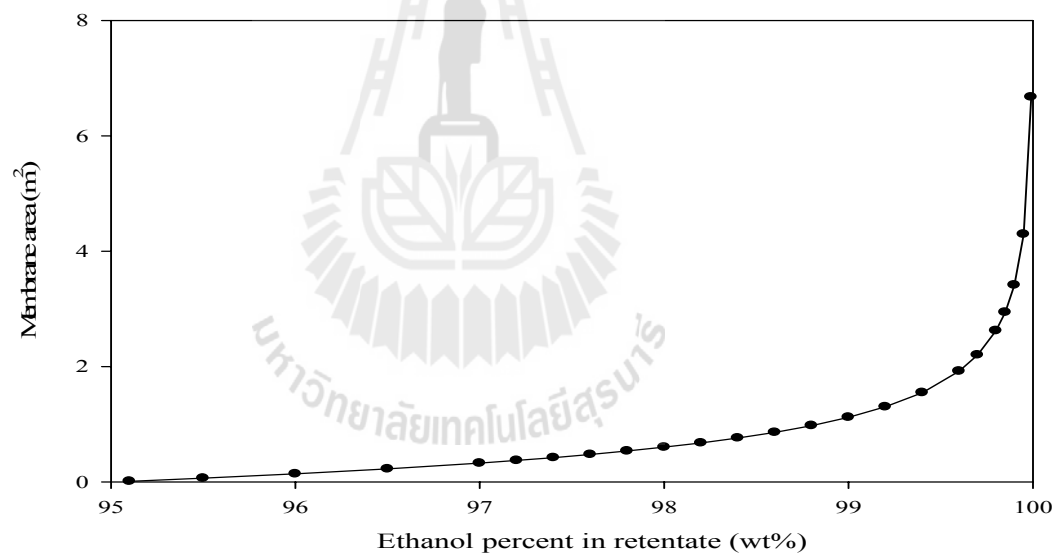


Figure 4.18 Vapor permeation mathematical simulation of required purity on membrane area.

The membrane area which is required to obtain a specified product purity will have an important impact on the cost of a membrane based separation process. Figure 4.18 showed the simulation of required membrane area as a function

of the ethanol purity in the retentate using the equation (22). For example of the calculation, the average separation factor was set at 100, initial feed ethanol concentration was 95 wt%, total permeation flux across the membrane was $1 \text{ kg.m}^{-2} \text{ h}^{-1}$ and mass flow rate of the ethanol was 0.1 kg.h^{-1} , respectively. Ranging from 95.1 to 99 wt% purity of ethanol, the required membrane area gradually increased with the increasing purity of ethanol in the retentate stream until the value reached approximately 1.12 m^2 when the purity of ethanol was about 99 wt%. However, the critical point could be observed when the retentate purity of ethanol exceeded this value. The required membrane area sharply increased from 1.12 to more than 6.67 m^2 when the purity of ethanol in the retentate stream increased from 99 to 99.99 wt%. The membrane area increased for nearly 6 times which reflected the substantially increased in investment cost. Therefore, it was reasonable to employ vapor permeation system to obtain ethanol content in retentate at 99 wt% since purification become much less attractive. Alternative technique which worked better at lower water concentration was more interesting. Adsorption was already employed in industrial scale dehydration process; however, the effect of initial water content in the feed had never been published before.

4.3 Adsorption

For adsorption experiment, adsorption beds packed with molecular sieve 3Å were used as the final step to dehydrate ethanol vapor with the objective of the highest purity for up to 99.95 wt%. Various concentrations of the feed ethanol increased from 95 to 99.0 wt% and feed pressure gage from 1 to 3 bars. In this work, operating parameters on adsorption capability and on productivity were investigated including the effect of feed ethanol concentrations and feed pressures.

4.3.1 Effect of feed gage pressure (Pg) on adsorption capability

Figure 4.19 showed the effect of feed gage pressure (Pg) on adsorption capability. The adsorbed masses of water increased with increasing feed gage pressure from 1 to 3 bars. It can be seen that, at higher feed gage pressure, the adsorbed quantity of water went down faster than lower feed gage pressure. From the experimental results, adsorption works much better at higher feed gage pressure.

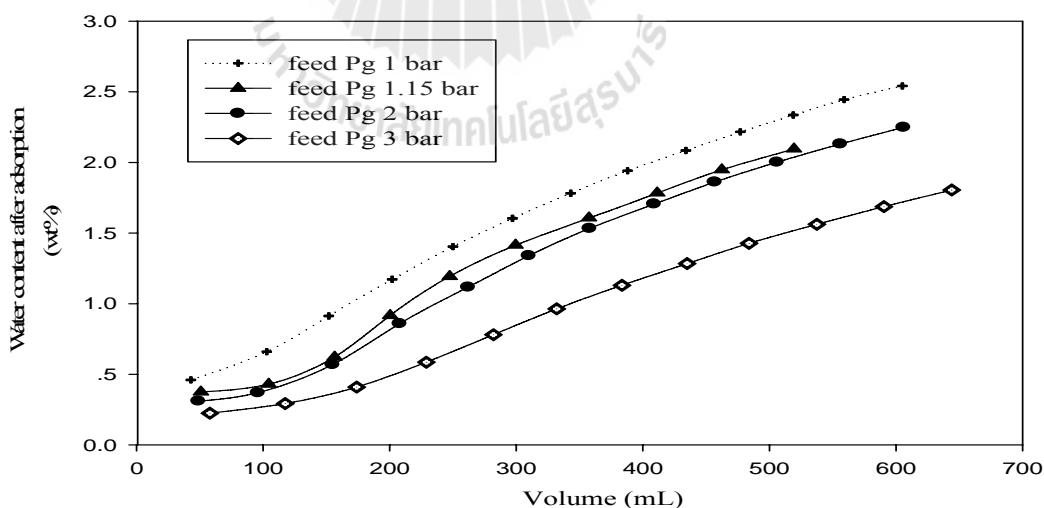


Figure 4.19 The relationship between wt% of water content after adsorption and volume; feed 95 wt% ethanol and column temperature of 145 °C.

4.3.2 Effect of feed ethanol concentrations on adsorption capability

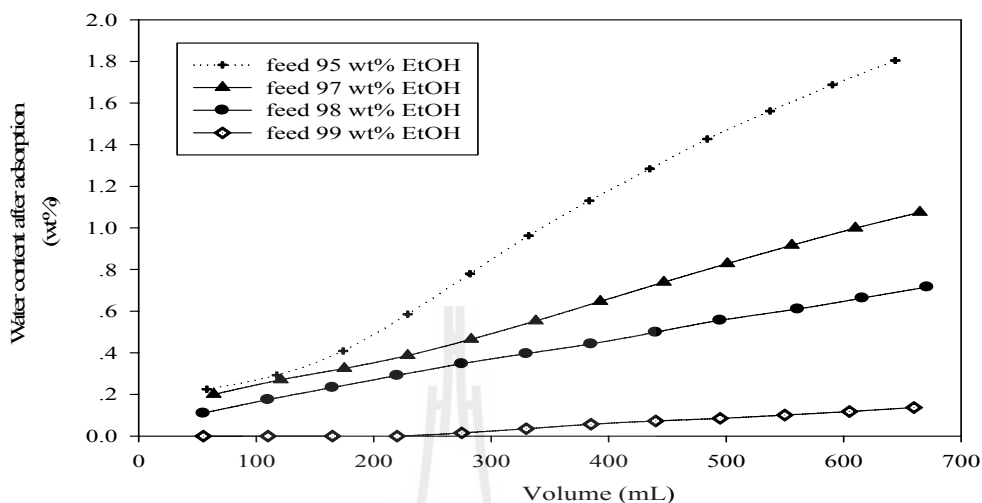


Figure 4.20 The relationship between wt% of water after adsorption and volume; feed gage pressure 3 bars and column temperature of 145 °C.

The effects of feed ethanol concentration on adsorption capability and on productivity were shown in Figures 4.20. Various concentrations of the feed ethanol increased from 95 to 99 wt%. Experimental results revealed that adsorption capability significantly changed at various feed concentration. At 95 wt% feed concentration, the water content of the ethanol product sharply increased just after only 100 mL with the lowest water content of approximately 0.29 wt%. This run was considered as a low performance because only small fraction of anhydrous ethanol was obtained. For 97 and 98 wt%, the correlation followed the same trend as the first run. In general, the slope was gradually increased with the increasing feed ethanol concentration. It was noted that, at the feed ethanol concentration of 99.0 wt %, the adsorption capability was the largest. From the experimental results, adsorption

process performed much better at this low water content. Residual water content went down to ppm level before gradually increased after 300 mL of accumulation. At 550 mL, the water content still at very low level of approximately 0.10 wt%. In comparison with the Figure 4.18, the experimental results confirmed that VP process worked better at higher water content in the feed whereas adsorption preferred lower water content. Because the adsorption capacity was strongly depended on the available sites for water molecules of molecular sieve, initial water content in the feed should be as low as possible. It was recommended that VP system should be employed to separate water until its concentration reached 1 wt% before entering the subsequent adsorption process.

4.4 Hybrid vapor permeation and pressure swing adsorption system

Figure 4.21 revealed experimental results of the dehydration performance by using hybrid VP and PSA system. The experiments were carried out at different flow rates of the ethanol product. Experimental results showed that the effect of flow rate had a profound effect on water content of the ethanol product. At the flow rate of 16.10 mL.min⁻¹, water content constantly increased since the beginning of the experiment. The slope was estimated to be approximately 0.08 wt% per 100 mL of the product. The best experimental result was obtained at the volumetric flow rate of 4.10 mL.min⁻¹. Although the lowest water content was lower than the best result observed in Figure 4.20, the value of 0.2 wt% was considered as an excellent experimental result. The water content of lower than 0.26 wt% was obtained for over 800 mL of the ethanol product. For continuous operation, when the water content exceeded the set point, dehydration must be switch to the other bed whilst the

saturated bed entered regeneration step. In order to maximize the volumetric flow rate of the desired purity of the ethanol product, additional experiments should be carried out for the relationship between volumetric flow rate, and regeneration time to establish the time for one cycle.

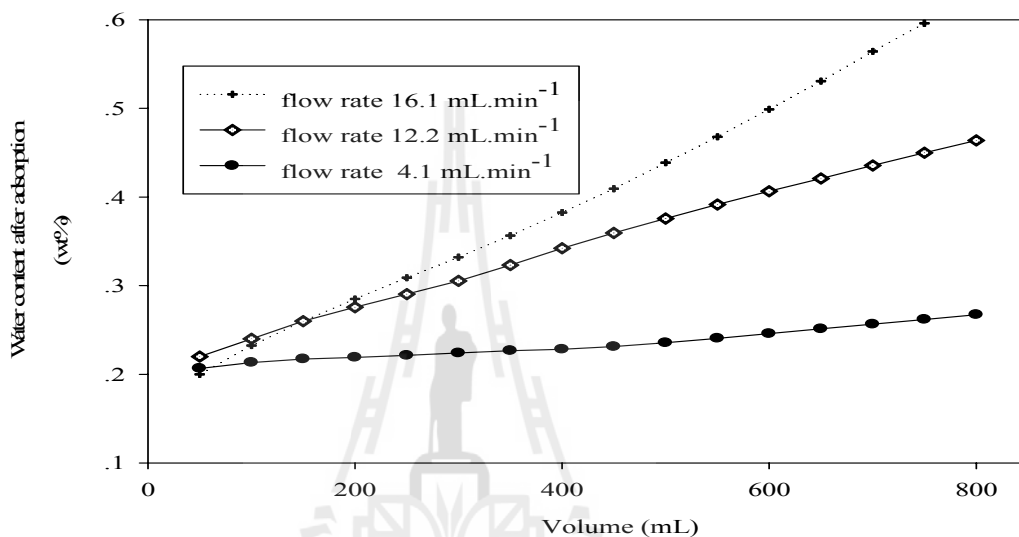


Figure 4.21 Effect of volumetric flow rate on residual water content during dehydration process by using hybrid VP + PSA system. Feed pressure 3 bars, feed ethanol concentration 95 wt%, and temperature 145 °C.

CHAPTER V

CONCLUSIONS

A major challenge in the dehydration of ethanol is the high energy cost associated with the separation of ethanol from the large excess of water. In addition, it forms azeotropic mixture at 95.6 wt% in which no more separation occurs using conventional heat treatment. Hybrid distillation, vapor permeation and pressure swing adsorption had been proposed as alternative technologies for azeotropic separation problems. A high efficiency continuous distillation column using forced-mixing concept was successfully developed at the Suranaree University of Technology (SUT). The highest purity ethanol concentration of 95 wt% ethanol was obtained at the optimum of stirrer speed of about 1,000 rpm.

For vapor permeation technique, the performance of water across the selective layer depends on many operating parameters including partial feed pressure, module temperature, retentate flow rate, and down stream pressure. In this work, a composite PVA/PAN membrane and NaA zeolite membrane on asymmetric porous support can be expected to be utilized in motor fuel grade ethanol (MFGE) production. For a composite PVA/PAN membrane, the highest purity of ethanol concentration of 99.16 wt% ethanol was achieved with the following operating conditions: module temperature 120 °C, retentate flow rate 0.875 mL.min⁻¹, 6 mbar vacuum pressure and feed pressure 1.6 bar. For NaA zeolite membrane, purity of ethanol concentration at 99 wt% ethanol was obtained with the following operating conditions:

module temperature 145 °C, retentate flow rate 7.785 mL.min⁻¹, 6 mbar vacuum pressure and feed pressure 3 bars. Comparing a composite PVA/PAN membrane and NaA zeolite membrane, the results suggested that NaA zeolite membrane had advantages over a composite PVA/PAN membrane in terms of separation factors and have an excellent thermal and chemical properties which mean that the commercial NaA zeolite membrane was higher membrane performance. The mathematical simulation suggested that membrane area increased exponentially with the required purity of ethanol. The membrane area increased for nearly 6 times when the purity of ethanol in the retentate stream increased from 99 to 99.99 wt%. Therefore, it was reasonable to employ vapor permeation system to obtain water content in retentate at 99 wt% since separation become much less effective.

For adsorption system, pressurized beds packed with molecular sieve 3Å (individual bed volume of 3.75 L) was used as the final step to dehydrate ethanol vapor for up to 99.99 wt%. The adsorption capacity of 3-Å molecular sieves for ethanol dehydration was investigated on lab scale apparatus. The masses of water and ethanol adsorbed were measured for various feed ethanol concentrations and operating feed pressure. From the experimental results, it could be concluded that adsorption worked much better at higher feed gage pressure and at lower water content, incidently at 1 wt% water content of the feed.

For the dehydration performance by using hybrid VP and PSA system, the water content of lower than 0.26 wt% for over 800 mL of the ethanol product was obtained with the following operating conditions: flow rate 4.10 mL.min⁻¹, feed gage pressure 3 bars, feed ethanol concentration 95 wt%, and module temperature 145 °C.

REFERENCES

- A.E. Jansen, W.F. Versteeg, B. van Engelenburg, J.H. Hanemaaijer and B.Ph. ter Meulen. (1992). Methods to improve flux during alcohol/water azeotrope separation by vapor permeation, **Journal of Membrane Science**. 68: 229-239.
- Banat, F.A., Abu Al-Rub, F.A., Simandl, J. (2000). Analysis of vapor-liquid equilibrium of ethanol-water system via headspace gas chromatography: effect of molecular sieves. **Separation and Purification Technology**. 18 (2): 111-118.
- Boontawan A., Bösch P., Schausberger, P., Brinkmann, T. and Friedl A. (2007). Dehydration of Ethanol/Water, Mixtures using Pervaporation and Vapor Permeation Technique, **Journal of Applied Membrane Science and Technology**. 5: 1-7.
- Boontawan A., เครื่องกลั่นประสิทธิภาพสูงด้วยระบบการปั่นผสมไอน้ำแบบต่อเนื่อง เลขที่คำขอ 1001000226 วันที่ 8 กุมภาพันธ์ 2553.
- C.K. Yeom, K.-H. Lee. (1997). Vapor permeation of ethanol-water mixtures using sodium alginate membranes with crosslinking gradient structure. **Journal of Membrane Science**. 135: 225-235.
- Delgado, P., Sanz, M.T., and Beltran S. (2008). Pervaporation study for different binary mixtures in the esterification system of lactic acid with ethanol, **Separation and Purification Technology**. 64:78-87.

- D.W. Breck, Zeolite Molecular Sieve, John Wiley & Sons Inc., 1974, p. 771.
- Fáunderz, C.A., Alvarez, V.H., & Valderrama, J.O., Predictive models to describe VLE in ternary mixtures water + ethanol + congener for wine distillation, *Thermochimica Acta*, 450, 110-117, 2006.
- Hartline, F. F. (1979). **Science (Washington, O.C.)**. 6: 41
- Hassaballah, A.A., Hills, J.H. (1990). Drying of ethanol vapors by adsorption on corn meal. **Biotechnol. Bioeng.** 35: 598–608.
- Huang, R.Y.M. (1991). Pervaporation Membrane Separation Process, Elsevier, USA.
- Jae-Hwa Chang, Je-Kang Yoo, Seung-Ho Ahn, Kyu-Hyun Lee and Suk-Moon Ko. (1998). Simulation of pervaporation process for ethanol dehydration by using pilot test results. **Korean J. Chem Eng.** 15(1): 28-36.
- Jan B. Haelssig, André Y. Tremblay, and Jules Thibault. (2008). Technical and Economic Considerations for Various Recovery Schemes in Ethanol Production by Fermentation. **Ind. Eng. Chem. Res.** 47: 6185–6191.
- Jianyu Guan and Xijun Hub (2003). Simulation and analysis of pressure swing adsorption: ethanol drying process by the electrical analogue. **Separation and Purification Technology**, 31: 31-35
- Marian Simo, Christopher J. Brown , Vladimir Hlavacek. (2008). Simulation of pressure swing adsorption in fuel ethanol production process . **Computers and Chemical Engineering**. 32: 1635–1649.
- Matsuura, T. (1994). Synthetic Membrane and Membrane Separation processes. **CRC Press, Florida.**

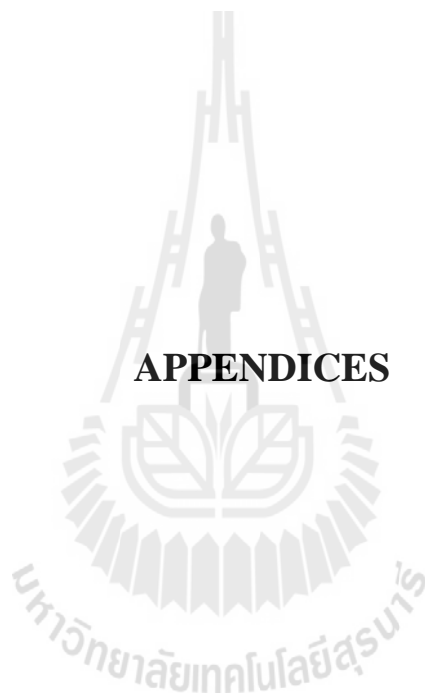
- M.J. Carmo and J.C. Gubulin. (1997). Ethanol-water adsorption on commercial 3Å zeolites: kinetic and thermodynamic data. **Braz. J. Chem. Eng.** vol. 14 no. 3.
- M.S. Schehlmann, E. Wiedemann, R.N. Lichtenthaler. (1995). Pervaporation and vapor permeation at the azeotropic point or in the vicinity of the LLE boundary phases of organic/aqueous mixtures. **Journal of Membrane Science.** 107: 277-282.
- Ohe, S., Vapor-Liquid Equilibrium Data, Elsevier, Amsterdam, 1989.
- Patricia M. Hoch and Jose ´ Espinosa. (2008). Conceptual Design and Simulation Tools Applied to the Evolutionary Optimization of a Bioethanol Purification Plant. **Ind. Eng. Chem. Res.** 47: 7381–7389.
- R. Rautenbach and F.P. Helmus, Some considerations on mass transfer resistances in solution-diffusion-type membrane processes, **J. Membrane Sci.**, 87 (1994) 171-181.
- Ried, R.C., J.M. Prausnitz, and B.E. Poling. (2000). The properties of gases and liquids. **McGraw Hill**.
- Roehr, M., 2001. The Biotechnology of Ethanol: Classical and Future Applications. WILEY-VCH, Germany.
- Seader, J.D. and E.J. Henley, Separation Process Principles. (2005). John Wiley & Sons, United Kingdom.
- Sato, K.; Sugimoto, K.; Nakane, T. (2008). Preparation of higher flux NaA zeolite membrane on asymmetric porous support and permeation behavior at higher temperatures up to 145 °C in vapor permeation. **Journal of Membrane Science.** 307, (2): 181-195.

- Shivaji Sircar. (2002). Pressure Swing Adsorption. **Ind. Eng. Chem. Res.** 41: 1389-1392.
- Thu Lan Thi Nguyen, Shabbir H. Gheewala, and Savitri Garivait. (2007). Full Chain Energy Analysis of Fuel Ethanol from Cassava in Thailand. **Environ. Sci. Technol.** 41: 4135-4142
- Torbjorn Pettersen, Kristian M. Lien. (1995). Design of hybrid distillation and vapor permeation processes. **Journal of Membrane Science.** 99: 21-30.
- Vicente Gomis, Ricardo Pedraza, Olga France ´s, Alicia Font, and Juan Carlos Asensi. (2007). Dehydration of Ethanol Using Azeotropic Distillation with Isooctane. **Ind. Eng. Chem. Res.** 46: 4572-4576.
- Wah Koon Teo and Douglas M. Ruthven. (1986). Adsorption of Water from Aqueous Ethanol Using 3-A Molecular Sieves. **Ind. Eng. Chem. Process Des. Dev.** 25: 17-21.
- Warren L. McCabe, Julian C. Smith and Peter Harriott. (2005). Unit operations of chemical engineering. Seventh edition. McGraw-Hill international edition. P-690.
- William L. Luyben. (2009). Control of a Column/Pervaporation Process for Separating the Ethanol/Water Azeotrope. **Ind. Eng. Chem. Res.** 48: 3484-3495.
- Yeom, C.K., and K.-H. Lee. (1997). Vapor permeation of ethanol-water mixtures using sodium alginate membranes with crosslinking gradient structure. **Journal of Membrane Science.** 135: 225-235.

Zhengbao Wang, Qinqin Ge, Jia Shao, and Yushan Yan. (2009). High Performance Zeolite LTA Pervaporation Membranes on Ceramic Hollow Fibers by Dipcoating-Wiping Seed Deposition. **J. AM. CHEM. SOC.** 131: 6910–6911.



APPENDICES



APPENDIX A

Table A-1 Boiling points of H₂O and Ethanol at different pressures.

Pressure (mbar)	Boiling point (°C)	
	Water	Ethanol
1	-22.5	-33.6
2.5	-11.7	-23.6
5	-2.7	-15.3
10	7.0	-6.4
25	21.1	6.5
50	32.9	17.3
100	45.8	29.1
250	65.0	46.5
500	81.4	61.4
1000	99.7	78.0
2000	120.3	96.0
5000	151.9	125.4
10000	180.0	150.9
20000	212.4	180.7

APPENDIX B

Table B-1 Vapor permeation mathematical simulation of required purity on membrane area from equation 22.

Ethanol in retentate (wt%)	Water in retentate (wt%)	Weight fraction of ethanol in retentate	Weight fraction of water in retentate	Membrane area (m ²)
95.10	4.90	0.9510	0.0490	0.013
95.50	4.50	0.9550	0.0450	0.066
96.00	4.00	0.9600	0.0400	0.141
96.50	3.50	0.9650	0.0350	0.226
97.00	3.00	0.9700	0.0300	0.327
97.20	2.80	0.9720	0.0280	0.373
97.40	2.60	0.9740	0.0260	0.422
97.60	2.40	0.9760	0.0240	0.476
97.80	2.20	0.9780	0.0220	0.536
98.00	2.00	0.9800	0.0200	0.603
98.20	1.80	0.9820	0.0180	0.677
98.40	1.60	0.9840	0.0160	0.762
98.60	1.40	0.9860	0.0140	0.861
98.80	1.20	0.9880	0.0120	0.978
99.00	1.00	0.9900	0.0100	1.121
99.20	0.80	0.9920	0.0080	1.303
99.40	0.60	0.9940	0.0060	1.550

Table B-1 (Continued).

Ethanol in retentate (wt%)	Water in retentate (wt%)	Weight fraction of ethanol in retentate	Weight fraction of water in retentate	Membrane area (m ²)
99.60	0.40	0.9960	0.0040	1.921
99.70	0.30	0.9970	0.0030	2.202
99.80	0.20	0.9980	0.0020	2.624
99.85	0.15	0.9985	0.0015	2.941
99.90	0.10	0.9990	0.0010	3.414
99.95	0.05	0.9995	0.0005	4.294
99.99	0.01	0.9999	0.0001	6.672

Remark:

n_f : mass flow rate (kg.h ⁻¹)	0.5
$\bar{\alpha}$: separation factor	100
w_f : water mass fraction in feed	0.05
J_p : total permeation flux across the membrane (kg.m ⁻² h ⁻¹)	1

Example of vapor permeation mathematical simulation of required purity on membrane area calculation.

from equation 22,
$$A = \frac{n_f \left[1 - \exp \left(\frac{1}{\bar{\alpha} - 1} \left(\ln \frac{w_r}{w_f} - \bar{\alpha} \ln \frac{1 - w_r}{1 - w_f} \right) \right) \right]}{\frac{J_p(w_f) - J_p(w_r)}{\ln \frac{J_p(w_f)}{J_p(w_r)}}$$

Where,	n_f : mass flow rate (kg.h ⁻¹)	0.5
	$\bar{\alpha}$: separation factor	100
	w_f : water mass fraction in feed	0.05
	w_r : water mass fraction in feed	0.049
	J_p : total permeation flux across the membrane (kg.m ⁻² h ⁻¹)	1

when $\ln \frac{w_r}{w_f} = \ln \frac{0.049}{0.05}$

$$= -0.020$$

$$\alpha \ln \frac{1-w_r}{1-w_f} = (100) \ln \frac{1-0.049}{1-0.05}$$

$$= -0.105$$

$$\frac{J_p(w_f) - J_p(w_r)}{\ln \frac{J_p(w_f)}{J_p(w_r)}} = \frac{(1)(0.05) - (1)(0.049)}{\ln \frac{(1)(0.05)}{(1)(0.049)}}$$

$$= 0.0495$$

Substitute the value in equation 22,

$$A = \frac{(0.5) \left[1 - \exp \left(\frac{1}{100-1} \right) (-0.02 - 0.105) \right]}{0.0495}$$

$$= 0.013 \text{ m}^2$$

APPENDIX C

Forced-mixing distillation

Table C-1 Shown distillation results.

Feed flowrate (mL.min⁻¹)	Feed composition (wt% ethanol)	Heat duty no.	Speed stirrer (rpm)	Product flowrate (mL.h⁻¹)	Product composition (wt% ethanol)
1.395	12	4	1446	532.32	93.00
1.395	12	4	1003	465.12	94.40
1.395	12	4	806	220.36	92.25
1.395	12	5	1446	540.50	93.50
1.395	12	5	1003	460.00	94.30
1.395	12	5	806	223.32	92.00
1.395	8	4	1446	115.52	93.00
1.395	8	4	1003	146.03	93.00
1.395	8	4	806	107.76	90.00
1.395	8	5	1446	110.18	90.00
1.395	8	5	1003	222.00	93.25
1.395	8	5	806	75.45	88.90
1.395	8	6	1446	115.68	90.00
1.395	8	6	1003	122.55	93.25
1.395	8	6	806	85.41	90.00
3.214	12	4	1446	550.5	94.30
3.214	12	4	1003	465.12	95.00

Table C-1 (continued)

Feed flowrate (mL.min ⁻¹)	Feed composition (wt% ethanol)	Heat duty no.	Speed stirrer (rpm)	Product flowrate (mL.h ⁻¹)	Product composition (wt% ethanol)
3.214	12	4	1003	465.12	95.00
3.214	12	4	806	310.25	93.25
3.214	12	5	1446	560.52	94.00
3.214	12	5	1003	500.00	95.00
3.214	12	5	806	320.15	93.25
3.214	8	4	1446	220.16	93.00
3.214	8	4	1003	384.84	94.80
3.214	8	4	806	163.30	93.00
3.214	8	5	1446	245.97	93.00
3.214	8	5	1003	383.42	94.00
3.214	8	5	806	110.00	92.00
3.214	8	6	1446	230.00	93.00
3.214	8	6	1003	300.27	93.80
3.214	8	6	806	102.62	92.25

Table C -2 Pure components parameters: van der Waals properties of r_i and q_i , and Antoine's equation constants A_i , B_i , and C_i [2].

Compounds	r_i	q_i	Antoine constants		
			A	B	C
Ethanol (1)	2.1055	1.9720	7.1688	1552.60	222.42
Water (2)	0.9200	1.4000	7.0436	1636.91	224.92

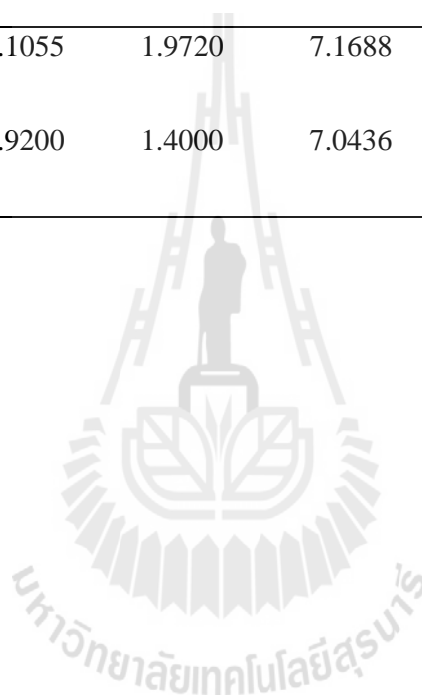


Table C-3 Experimental VLE data from forced-mixing distillation corresponding to equilibrium of the binary ethanol/water mixtures at atmospheric pressure; liquid phase mole fraction (x), vapor phase mole fraction (y), liquid temperature ($^{\circ}\text{C}$), and relative volatility (α), respectively.

Temperature ($^{\circ}\text{C}$)	$x_{ethanol}$	x_{water}	$y_{ethanol}$	y_{water}	α
99.7	0	1	0	1	-
99.0	0.004	0.996	0.735	0.265	690.62
98.3	0.017	0.983	0.876	0.124	408.50
97.5	0.031	0.969	0.881	0.119	231.41
95.3	0.039	0.961	0.894	0.106	207.82
94.6	0.05	0.95	0.894	0.106	160.25
94.0	0.053	0.947	0.894	0.106	150.70
93.2	0.056	0.944	0.894	0.106	142.17
91.6	0.067	0.933	0.894	0.106	117.45
90.1	0.069	0.931	0.894	0.106	113.80
88.4	0.074	0.926	0.894	0.106	105.54
85.3	0.132	0.868	0.894	0.106	55.46
84.8	0.144	0.856	0.894	0.106	50.14
83.7	0.207	0.793	0.894	0.106	32.31
82.7	0.281	0.719	0.894	0.106	21.58
81.0	0.37	0.63	0.894	0.106	14.36
80.2	0.477	0.523	0.894	0.106	9.25

Table C-3 (continued)

Temperature (°C)	$x_{ethanol}$	x_{water}	$y_{ethanol}$	y_{water}	α
79.1	0.61	0.39	0.894	0.106	5.39
78.1	0.779	0.221	0.894	0.106	2.39
78.1	0.881	0.119	0.894	0.106	1.14
78.1	0.895	0.105	0.895	0.105	1.00



APPENDIX D

Vapor permeation

(The hydrophilic PVA/PAN-composite membrane)

Example of logarithmic mean and separation factor calculation.

From table D-1 at cell temperature of 80 °C,

ethanol concentration in feed (wt%)	95
water concentration in retentate (wt%)	5.610
ethanol concentration in retentate (wt%)	94.390
water concentration in permeate (wt%)	12.411
ethanol concentration in permeate (wt%)	87.589

From logarithmic mean of feed ethanol concentration or [Feed ethanol]_{LM}

$$\begin{aligned}
 &= \frac{W_r, \text{ethanol} - W_f, \text{ethanol}}{\ln \frac{W_r, \text{ethanol}}{W_f, \text{ethanol}}} \\
 &= \frac{0.9439 - 0.95}{\ln \frac{0.9439}{0.95}} \\
 &= \mathbf{0.94695}
 \end{aligned}$$

So, [Feed ethanol]_{LM} in table D-1 at cell temperature of 80 °C was 94.695 wt%.

$$\begin{aligned}
 \text{From separation factor or } \alpha &= \frac{W_P, \text{water} / W_f, \text{water}}{W_P, \text{ethanol} / W_f, \text{ethanol}} \\
 &= \frac{0.12411 / (1 - 0.94695)}{0.87589 / 0.94695} \\
 \alpha &= \mathbf{2.529}
 \end{aligned}$$

Table D-1 The values of concentration of water, ethanol in retentate and permeate stream, flux and α with cell temperature, of polymeric PVA/PAN-composite membrane; feed gage pressure (P_g) of 1.4 bar, feed concentration of ethanol 95 wt% and flow rate $0.95 \text{ mL}\cdot\text{min}^{-1}$.

Cell temperature (°C)	Concentration (wt%)				Flux ($\text{kg}\cdot\text{m}^{-2}\cdot\text{h}^{-1}$)			[Feed ethanol] _{LM}	α
	Retentate		Permeate		Total	Water	Ethanol		
	Water	Ethanol	Water	Etahnol					
80	5.610	94.390	12.411	87.589	1.311	0.131	1.18	94.695	2.529
90	5.258	94.742	11.655	88.345	1.282	0.120	1.162	94.871	2.440
100	3.068	96.932	12.223	87.777	1.476	0.145	1.331	95.963	3.310
110	1.173	98.827	10.325	89.675	1.013	0.084	0.929	96.901	3.600
120	0.844	99.156	15.185	84.815	1.264	0.156	1.108	97.063	5.917

Table D-2 The values of concentration of water, ethanol in retentate and permeate stream, flux and α with flow rates of polymeric PVA/PAN-composite membrane; feed gage pressure (P_g) 1.6 bar, feed concentration of ethanol 95 wt% and cell temperature of 120 °C.

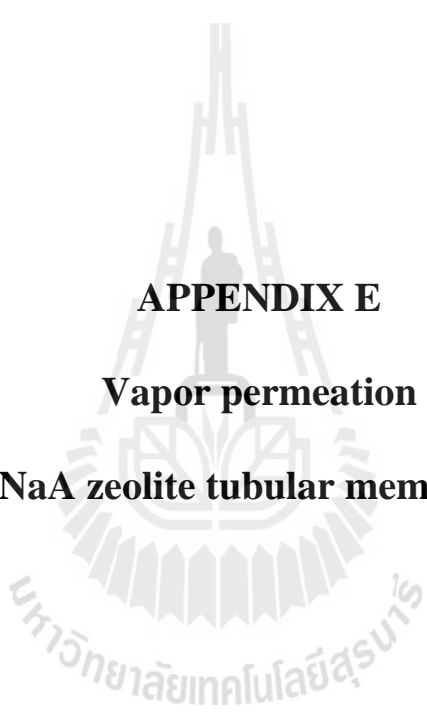
Flow rate (mL.min ⁻¹)	Concentration (wt%)				Flux (kg.m ⁻² .h ⁻¹)			[Feed ethanol] _{LM}	α
	Retentate		Permeate		Total	Water	Ethanol		
	Water	Ethanol	Water	Ethanol					
0.875	0.844	99.156	15.185	84.815	1.264	0.156	1.108	97.063	5.917
1.867	1.565	98.435	19.880	80.120	1.366	0.222	1.143	96.708	7.288
2.500	2.602	97.398	21.644	78.356	1.474	0.263	1.212	96.194	6.981
3.025	2.761	97.239	24.045	75.955	1.575	0.313	1.262	96.115	7.832

Table D-3 The values of concentration of water, ethanol in retentate and permeate stream, flux and α with feed gage pressure (P_g) of polymeric PVA/PAN-composite membrane; flow rate of $1.85 \text{ mL}\cdot\text{min}^{-1}$, feed concentration of ethanol 95 wt% and cell temperature of $120 \text{ }^\circ\text{C}$.

P_g (bar)	Concentration (wt%)				Flux ($\text{kg}\cdot\text{m}^{-2}\cdot\text{h}^{-1}$)			[Feed ethanol] _{LM}	α
	Retentate		Permeate		Total	Water	Ethanol		
	Water	Ethanol	Water	Ethanol					
1.2	3.179	96.821	20.764	79.236	1.190	0.203	0.987	95.908	6.141
1.35	2.044	97.956	19.438	80.562	1.081	0.172	0.909	96.470	6.595
1.4	1.758	98.352	16.526	83.474	0.989	0.133	0.856	96.666	5.741
1.6	1.565	98.435	19.880	80.120	1.366	0.222	1.143	96.708	7.288
1.8	1.145	98.855	21.863	78.137	1.383	0.249	1.134	96.915	8.789

Table D-4 The values of concentration of water, ethanol in retentate and permeate stream, flux and α with flow rates of polymeric PVA/PAN-composite membrane; feed gage pressure (P_g) of 0.75 bar, feed concentration of ethanol 95 wt% and cell temperature of 80 °C.

Flow rate (mL.min ⁻¹)	Concentration (wt%)				Flux (kg.m ⁻² .h ⁻¹)			[Feed ethanol] _{LM}	α
	Retentate		Permeate		Total	Water	Ethanol		
	Water	Ethanol	Water	Ethanol					
2.067	3.179	96.821	14.960	85.040	0.899	0.109	0.790	95.908	4.123
2.675	4.426	95.574	18.549	81.451	1.114	0.169	0.945	95.287	4.604
12.667	5.254	94.746	22.957	77.043	1.192	0.226	0.966	94.873	5.514
13.117	5.135	94.865	24.695	75.305	1.015	0.208	0.807	94.932	6.143



APPENDIX E
Vapor permeation
(NaA zeolite tubular membrane)

Table E-1 The values of concentration of water, ethanol in retentate and permeate stream, flux and α with feed gage pressure (P_g) of NaA zeolite tubular membrane; flow rate of $7.785 \text{ mL}\cdot\text{min}^{-1}$, feed concentration of ethanol 95 wt%, 6 mbar vacuum pressure and cell temperature of $145 \text{ }^\circ\text{C}$.

P_g (bar)	Concentration (wt%)				Flux ($\text{kg}\cdot\text{m}^{-2}\cdot\text{h}^{-1}$)			[Feed ethanol] _{LM}	α
	Retentate		Permeate		Total	Water	Ethanol		
	Water	Ethanol	Water	Ethanol					
0.4	3.166	96.834	97.368	2.632	0.339	0.328	0.011	95.885	861.780
0.8	2.248	97.752	85.032	14.968	0.449	0.367	0.082	96.340	149.553
1.2	1.918	98.082	86.444	13.556	0.530	0.442	0.088	96.504	176.005
2.0	1.523	98.477	90.616	9.384	0.673	0.594	0.079	96.699	282.859
2.4	1.287	98.713	91.966	8.034	1.001	0.900	0.100	96.815	347.987
3.0	1.104	98.896	92.090	7.910	1.089	0.982	0.107	96.905	364.551

Table E-2 The values of concentration of water, ethanol in retentate and permeate stream, flux and α with cell temperature of NaA zeolite tubular membrane; feed gage pressure 1.6 bar, feed concentration of ethanol 95 wt% and flow rate 8.77 mL.min⁻¹.

Cell temperature (°C)	Concentration (wt%)				Flux (kg.m ⁻² .h ⁻¹)			[Feed ethanol] _{LM}	α
	Retentate		Permeate		Total	Water	Ethanol		
	Water	Ethanol	Water	Ethanol					
110	2.538	97.462	71.835	28.165	0.864	0.576	0.288	96.197	64.507
120	2.381	97.619	71.836	28.164	0.868	0.579	0.289	96.274	65.906
135	1.985	98.015	76.829	23.171	0.814	0.588	0.226	96.471	90.626
145	1.852	98.148	83.611	16.390	0.701	0.561	0.140	96.536	142.176



Table E-3 The values of concentration of water, ethanol in retentate and permeate stream, flux and α with flow rates of NaA zeolite tubular membrane; feed gage pressure (P_g) 1.6 bar, feed concentration of ethanol 95 wt%, 6 mbar vacuum pressure and cell temperature of 145 °C.

Flow rate (mL.min ⁻¹)	Concentration (wt%)				Flux (kg.m ⁻² .h ⁻¹)			[Feed ethanol] _{LM}	α
	Retentate		Permeate		Total	Water	Ethanol		
	Water	Ethanol	Water	Ethanol					
5.167	1.457	98.543	86.444	13.556	0.174	0.145	0.029	96.601	181.242
6.033	1.720	98.280	87.845	12.155	0.480	0.408	0.072	96.731	213.882
8.867	1.852	98.148	83.610	16.390	0.701	0.561	0.140	96.536	142.176
16.667	3.166	96.834	89.235	10.765	0.977	0.847	0.130	95.885	193.143
21.833	3.647	96.3543	90.616	9.384	1.107	0.978	0.129	95.646	212.127

Table E-4 The values of concentration of water, ethanol in retentate and permeate stream, flux and α with flow rates of NaA zeolite tubular membrane; feed gage pressure (P_g) 1.6 bar, feed concentration of ethanol 95 wt%, 6 mbar vacuum pressure and cell temperature of 120 °C.

Flow rate (mL.min ⁻¹)	Concentration (wt%)				Flux (kg.m ⁻² .h ⁻¹)			[Feed ethanol] _{LM}	α
	Retentate		Permeate		Total	Water	Ethanol		
	Water	Ethanol	Water	Ethanol					
7.767	2.467	97.533	64.099	35.901	0.821	0.479	0.342	96.232	45.594
7.933	2.072	97.928	68.778	31.222	0.840	0.532	0.308	96.427	59.455
8.767	2.379	97.621	71.836	28.164	0.868	0.579	0.289	96.275	65.929
11.300	2.554	97.446	73.348	26.652	0.942	0.644	0.298	96.188	69.450
14.867	2.992	97.008	74.099	25.901	1.152	0.797	0.355	95.972	68.155

Table E-3 The values of concentration of water, ethanol in retentate and permeate stream, flux and α with flow rates of NaA zeolite tubular membrane; feed gage pressure (P_g) 1.6 bar, feed concentration of ethanol 95 wt%, 6 mbar vacuum pressure and cell temperature of 145 °C.

Flow rate (mL.min ⁻¹)	Concentration (wt%)				Flux (kg.m ⁻² .h ⁻¹)			[Feed ethanol] _{LM}	α
	Retentate		Permeate		Total	Water	Ethanol		
	Water	Ethanol	Water	Ethanol					
5.167	1.457	98.543	86.444	13.556	0.174	0.145	0.029	96.601	181.242
6.033	1.720	98.280	87.845	12.155	0.480	0.408	0.072	96.731	213.882
8.867	1.852	98.148	83.610	16.390	0.701	0.561	0.140	96.536	142.176
16.667	3.166	96.834	89.235	10.765	0.977	0.847	0.130	95.885	193.143
21.833	3.647	96.3543	90.616	9.384	1.107	0.978	0.129	95.646	212.127

APPENDIX F

Adsorption

Table F-1 The values of concentration of water and ethanol after adsorption with volume (mL); feed concentration of ethanol 95 wt%, column temperature of 145 °C and feed gage pressure 1 bar.

Feed pressure (bar)	Feed concentration of ethanol (wt%)	Volume of ethanol after adsorption (mL)	Water content after adsorption (wt%)	Ethanol content after adsorption (wt%)
1	95	43	0.460	99.540
1	95	103	0.660	99.340
1	95	152	0.913	99.087
1	95	202	1.173	98.828
1	95	250	1.404	98.596
1	95	297	1.604	98.396
1	95	343	1.782	98.218
1	95	388	1.941	98.059
1	95	434	2.084	97.916
1	95	477	2.216	97.784
1	95	519	2.336	97.664
1	95	559	2.445	97.555
1	95	605	2.541	97.459

Table F-2 The values of concentration of water and ethanol after adsorption with volume (mL); feed concentration of ethanol 95 wt%, column temperature of 145 °C and feed gage pressure 1.15 bars.

Feed pressure (bar)	Feed concentration of ethanol (wt%)	Volume of ethanol after adsorption (mL)	Water content after adsorption (wt%)	Ethanol content after adsorption (wt%)
1.15	95	51	0.375	99.625
1.15	95	104.5	0.430	99.570
1.15	95	156.5	0.622	99.378
1.15	95	200.5	0.917	99.083
1.15	95	247.5	1.193	98.807
1.15	95	299.5	1.414	98.586
1.15	95	357.5	1.606	98.394
1.15	95	411.5	1.784	98.216
1.15	95	462.5	1.948	98.052
1.15	95	519.5	2.095	97.905

Table F-3 The values of concentration of water and ethanol after adsorption with volume (mL); feed concentration of ethanol 95 wt%, column temperature of 145 °C and feed gage pressure 2 bars.

Feed pressure (bar)	Feed concentration of ethanol (wt%)	Volume of ethanol after adsorption (mL)	Water content after adsorption (wt%)	Ethanol content after adsorption (wt%)
2	95	49	0.310	99.690
2	95	96	0.370	99.630
2	95	155	0.568	99.432
2	95	208	0.859	99.141
2	95	262	1.117	98.883
2	95	310	1.340	98.660
2	95	358	1.533	98.467
2	95	409	1.706	98.294
2	95	457	1.862	98.138
2	95	506	2.002	97.999
2	95	556.1	2.130	97.870
2	95	606.1	2.249	97.751

Table F-4 The values of concentration of water and ethanol after adsorption with volume (mL); feed concentration of ethanol 95 wt%, column temperature of 145 °C and feed gage pressure 3.0 bars.

Feed pressure (bar)	Feed concentration of ethanol (wt%)	Volume of ethanol after adsorption (mL)	Water content after adsorption (wt%)	Ethanol content after adsorption (wt%)
3.0	95	58	0.225	99.775
3.0	95	117.5	0.293	99.708
3.0	95	174	0.409	99.591
3.0	95	229	0.586	99.414
3.0	95	282	0.780	99.220
3.0	95	332	0.963	99.037
3.0	95	383.5	1.130	98.870
3.0	95	435	1.284	98.716
3.0	95	484	1.427	98.573
3.0	95	537.5	1.562	98.438
3.0	95	590.5	1.687	98.313
3.0	95	644	1.805	98.195

Table F-5 The values of concentration of water and ethanol after adsorption with volume (mL); feed concentration of ethanol 97 wt%, column temperature of 145 °C and feed gage pressure 3.0 bars.

Feed pressure (bar)	Feed concentration of ethanol (wt%)	Volume of ethanol after adsorption (mL)	Water content after adsorption (wt%)	Ethanol content after adsorption (wt%)
3.0	97	64	0.200	99.800
3.0	97	121	0.270	99.730
3.0	97	175	0.325	99.675
3.0	97	229	0.387	99.613
3.0	97	283	0.465	99.535
3.0	97	338	0.553	99.447
3.0	97	393	0.647	99.353
3.0	97	447	0.739	99.261
3.0	97	501	0.829	99.171
3.0	97	556	0.917	99.084
3.0	97	610	0.999	99.001
3.0	97	665	1.075	98.925

Table F-6 The values of concentration of water and ethanol after adsorption with volume (mL); feed concentration of ethanol 98 wt%, column temperature of 145 °C and feed gage pressure 3.0 bars.

Feed pressure (bar)	Feed concentration of ethanol (wt%)	Volume of ethanol after adsorption (mL)	Water content after adsorption (wt%)	Ethanol content after adsorption (wt%)
3.0	98	55	0.110	99.890
3.0	98	110	0.175	99.825
3.0	98	165	0.233	99.767
3.0	98	220	0.291	99.709
3.20	98	275	0.348	99.653
3.0	98	330	0.396	99.604
3.0	98	385	0.443	99.557
3.0	98	440	0.499	99.501
3.0	98	495	0.556	99.444
3.0	98	561	0.611	99.390
3.0	98	616	0.663	99.337
3.0	98	671	0.716	99.475

Table F-7 The values of concentration of water and ethanol after adsorption with volume (mL); feed concentration of ethanol 99 wt%, column temperature of 145 °C and feed gage pressure 3.0 bars.

Feed pressure (bar)	Feed concentration of ethanol (wt%)	Volume of ethanol after adsorption (mL)	Water content after adsorption (wt%)	Ethanol content after adsorption (wt%)
3.0	99	55	0.0	100.0
3.0	99	110	0.0	100.0
3.0	99	165	0.0	100.0
3.0	99	220	0.0	100.0
3.0	99	275	0.015	99.985
3.0	99	330	0.035	99.965
3.0	99	385	0.057	99.943
3.0	99	440	0.073	99.928
3.0	99	495	0.085	99.915
3.0	99	550	0.101	99.899
3.0	99	605	0.118	99.882
3.0	99	660	0.137	99.863



APPENDIX G

**Hybrid VP (NaA zeolite tubular membrane)
and PSA system**

Table G-1 The values of concentration of water and ethanol after adsorption with volume (mL); flow rate $19.26 \text{ mL}\cdot\text{min}^{-1}$ and column (PSA), cell (VP) temperature of $145 \text{ }^{\circ}\text{C}$.

Feed pressure (bar)	Feed concentration of ethanol (wt%)	Volume of ethanol after adsorption (mL)	Water content after adsorption (wt%)	Ethanol content after adsorption (wt%)
3	95	50	0.145	99.855
3	95	105	0.159	99.841
3	95	156	0.183	99.818
3	95	206	0.201	99.799
3	95	256	0.219	99.782
3	95	306	0.237	99.763
3	95	356	0.257	99.743
3	95	406	0.281	99.719
3	95	456	0.309	99.691
3	95	506	0.336	99.665
3	95	556	0.363	99.637
3	95	606	0.392	99.608
3	95	656	0.423	99.577
3	95	706	0.456	99.544
3	95	756	0.490	99.510
3	95	806	0.525	99.475

Table G-2 The values of concentration of water and ethanol after adsorption with volume (mL); flow rate $16.1 \text{ mL}\cdot\text{min}^{-1}$ and column (PSA), cell (VP) temperature of $145 \text{ }^{\circ}\text{C}$.

Feed pressure (bar)	Feed concentration of ethanol (wt%)	Volume of ethanol after adsorption (mL)	Water content after adsorption (wt%)	Ethanol content after adsorption (wt%)
3	95	50	0.200	99.800
3	95	100	0.233	99.768
3	95	150	0.260	99.740
3	95	200	0.285	99.715
3	95	250	0.309	99.691
3	95	300	0.332	99.668
3	95	350	0.356	99.644
3	95	400	0.383	99.618
3	95	450	0.409	99.591
3	95	500	0.439	99.561
3	95	550	0.468	99.532
3	95	600	0.499	99.501
3	95	650	0.531	99.469
3	95	700	0.564	99.436
3	95	750	0.596	99.404

Table G-3 The values of concentration of water and ethanol after adsorption with volume (mL); flow rate 12.20 mL.min⁻¹ and column (PSA), cell (VP) temperature of 145 °C.

Feed pressure (bar)	Feed concentration of ethanol (wt%)	Volume of ethanol after adsorption (mL)	Water content after adsorption (wt%)	Ethanol content after adsorption (wt%)
3	95	50	0.220	99.780
3	95	100	0.240	99.760
3	95	150	0.260	99.740
3	95	200	0.276	99.724
3	95	250	0.291	99.710
3	95	300	0.305	99.695
3	95	350	0.323	99.677
3	95	400	0.342	99.658
3	95	450	0.359	99.641
3	95	500	0.376	99.624
3	95	550	0.392	99.608
3	95	600	0.406	99.594
3	95	650	0.421	99.579
3	95	700	0.436	99.564
3	95	750	0.450	99.550
3	95	800	0.464	99.536

Table G-4 The values of concentration of water and ethanol after adsorption with volume (mL); flow rate 4.1 mL.min⁻¹ and column (PSA), cell (VP) temperature of 145 °C.

Feed pressure (bar)	Feed concentration of ethanol (wt%)	Volume of ethanol after adsorption (mL)	Water content after adsorption (wt%)	Ethanol content after adsorption (wt%)
3	95	50	0.207	99.793
3	95	100	0.213	99.787
3	95	150	0.217	99.783
3	95	200	0.219	99.781
3	95	250	0.221	99.779
3	95	300	0.224	99.776
3	95	350	0.227	99.773
3	95	400	0.228	99.772
3	95	450	0.231	99.769
3	95	500	0.236	99.764
3	95	550	0.241	99.759
3	95	600	0.246	99.754
3	95	650	0.251	99.749
3	95	700	0.257	99.743
3	95	750	0.262	99.738
3	95	800	0.267	99.733

BIOGRAPHY

Miss Saengduan Pimkaew was born on August 31, 1985 in Surin province. She obtained her Bachelor of Engineering degree in Chemical Engineering from School of Chemical Engineering, Institute of Engineering, Suranaree University of Technology in 2008. After that, she decided to further study master degree in the field of biotechnology. During study, she received financial support from the Suranaree University of Technology, Thailand under the project no.3-304-53-12-32. After she finished coursework, she worked as a research assistant in Biofuel Production from Biomass Research Unit, School of Biotechnology, Institute of Agricultural Technology, Suranaree University of Technology, Thailand. During this time she had practiced skills in the field of Membrane technology, Distillation, and Pressure Swing Adsorption (PSA) technique. Her research topic was “High quality Ethanol Production using Distillation, Vapor Permeation and Pressure Swing Adsorption (PSA) techniques”. The results from part of this study was presented at International Conference on Agriculture and Agro-Industry, November 19-20, 2010, Mae Fah Luang University, Chiang Rai, Thailand.